

Machine Learning Applications in Healthcare: A Deep Dive into CNN and ML Models for Breast Cancer, Lung Cancer, and COVID-19 Diagnosis

P. V. V.S. Srinivas¹, Yelleti Durga Sai Deepak², Nakka Hrushikesh Bhanu³, Velaga Hema Vardhan⁴, Karre Anirudh⁵

¹Department of Computer Science and Engineering, Koneru Lakshmaiah Education Foundation, Vaddeswaram 522502, Andhra Pradesh, India.

^{2,3,4,5}Department of Computer Science and Information Technology, Koneru Lakshmaiah Education Foundation, Vaddeswaram 522502, Andhra Pradesh, India.

¹cnu.pvvs@gmail.com, ²2100090151csit@gmail.com, ³2100090154csit@gmail.com,

⁴2100090027csit@gmail.com, ⁵2100090161csit@gmail.com

ARTICLE INFO	ABSTRACT
Received: 22 Dec 2024 Revised: 14 Feb 2025 Accepted: 26 Feb 2025	<p>Machine learning (ML) models have proven to be important tools in the diagnosis of multiple diseases in medicine. In this study, various algorithms like logistic regression, support vector machine (SVM), decision trees, typical models like XGboost or AdaBoost, and combination of neural networks for clustering is used. VGG-16, VGG et al., Deep Learning Architecture – 19, ResNet-50, and ResNet-101. Before being used for diagnostic, medical images are preprocessed to improve quality and achieve better outcome. Because CNNs have a deep hierarchical structure, each of its successful models adds a special contribution to the classification process of CNNs and the state-of-the-art inference variants. This study attempts to contrast the results and result performance of these models for breast cancer diagnosis, lung cancer diagnosis and COVID-19 diagnosis without specifying any accuracy. Machine learning models' integration into health analytics includes disease detection and treatment. Diagnostic criteria are different between each of the models that are used. Logistic regression, SVM, Decision Trees, XGBoost, and AdaBoost are a traditional model that helps us classify what we are doing and provide an efficient and effective result of production. Deep learning models, such as CNN, VGG-16, VGG-19, are on the other hand. ResNet-50 and ResNet-101 are able to do well processing high quality objects like medical images because they have features. It has powerful functionality and deep architecture. Medical applications are unique and capture the complex patterns in images. Assess cost and confirm performance.</p> <p>Keywords: Machine Learning, Breast Cancer, Lung Cancer, COVID-19, CNN, VGG-16, VGG-19, ResNet-50, ResNet-101, Support Vector Machine (SVM), Logistic Regression, Decision Tree, XGBoost, AdaBoost, Medical Image Classification, Deep Learning, Healthcare Diagnostics</p>

1. INTRODUCTION

ML in medicine is changing the way diseases such as breast cancer, lung cancer and COVID are diagnosed. Many types of medical data, especially medical images, play an especially important role in the diagnosis process, see Machine learning. These models aid the doctor in making faster and more accurate diagnosis of the complex data using these subtle patterns and inconsistency. In this work, convolutional neural network (CNN), VGG 16, VGG architecture, 19, ResNet 50, ResNet 101, as well as classical ML models were evaluated. Predictions and accuracy are enhanced via the advanced support methods including XGBoost and AdaBoost. Deep learning models particularly CNN and its variants such as VGG and ResNet, have been popular for its capacity to process many medical images. They have a deep structure which makes them good at capturing complex structures and pulling out the important features from good medical images, in particular

for the task of cancer diagnosis as well as early sign of COVID-19 problems. In this case, the training model and deep learning are going to be evaluated in diagnosing breast cancer, lung cancer and COVID-19. This research analyzes the strengths and weaknesses of each model to reveal the combination of traditional machine learning with deep learning technique yields accurate diagnostic tools. Such integration could represent a revolution in diagnostic tools, offering something better than faster, more accurate, and more personalized solutions for threats that kill mostly people, namely, disease.

2. RELATED WORK

Sun YS (2017) [1] made evaluation of risk factors and measures that can prevent breast cancer shows a lot of improved knowledge about the cause of the diseases. They also talk about breast cancer cells and genetics, and drug and biological prevention. These conclude that breast cancer should be detected at an early stage and more efforts should be made towards preventing it. Pamela Cowin (2005) [2] examined the hormonal changes of Cadherins and catenins in breast cancer and also explored the physiological operations of the two during breast cancer development. They observed that absences of E-cadherin manifestation is characteristic of the lobular form of breast cancer, in which it functions as an anti-cancer substance as well as being implicated in cancer prevention. This review also explores how β -catenin signaling is increased in over 50% of breast tumors and relates it to oncogenic genes via increased levels of mammary progenitor cells. M. Veta (2014) [3] Breast cancer histopathological image assessment techniques are discussed where focus is placed on whole slide imaging (WSI) approaches. They also establish the possibility of decreasing the laboratory disease load and improving the overall diagnostic sensitivity for most cancers of the female genital tract using image analysis tools. Topics addressed include tissue preprocessing, staining, digitization of slides, and available imaging methods for the diagnosis and prediction of breast cancer. Hassan and El-Shenawee (2011) [4] Discovered the different types of radiological equipments required for diagnosing breast cancer and understand why existing therapies are insufficient. They also presented an overview of the state-of-the-art cancer diagnostic technologies using microwave measurements for cancer detection, diffusion optical tomography for brain cancer, and MRI. The gap identified in the literature review is to provide biomedical researchers with detailed and broad knowledge of advancements in electromagnetic detection techniques for breast cancer detection. E. C. Fear (2003) [5] explores Microwave imaging is being studied to determine its potential to detect radiation distribution in tissue and physical structure. The authors explain that the changes in radioactivity to diagnose cancer in blood. Even in that use, they note that imaging has also been applied to monitoring hyperthermia; changes in electrical properties used to gauge the heat treatment which they say is an appalling, if topical, application of the technology for diagnosis. Z. Wang et al. (2019) [6] presents a computer aided diagnosis (CAD) system which enhances the accuracy of current technology by applying combined deep features of convolutional neural network (CNN). A robust system is developed through the use of an unsupervised cloud based machine (ELM) to combine deep features to morphology, texture and density to arrive at a large scale detection method. Roslidar et al. (2020) [7] It reviews recent advances in thermography and deep learning emphasizes the necessity to make an intervention in developing a noninvasive screening protocol. The potential for thermal imaging to detect early breast cancer by detecting breast temperature and use of neural networks, was also highlighted. S. B. Sakri. (2018) [8] multiple data mining algorithms for investigating breast cancer prognosis. In order to alleviate survivors' concerns about recovery, the study used classifiers such as Naive Bayes, K-Nearest Neighbors, and REPTree, but together with these, it utilized optimization techniques. The results demonstrate that this increases the accuracy of predicting models and leads to early treatment. Yari (2020) [9] Address breast cancer diagnosis challenge using limited clinical data by to explore the applications of deep learning. [10] proposed a deep learning method for the classification of breast cancer from pathological images and demonstrate its potential to alleviate the overfitting problem of existing CNNs with limited data. Next, they describe the first Alex Net-BC model, trained on the ImageNet dataset and then fine-tuned with breast clinical data. The authors introduce an advanced cross entropy loss function to reduce overconfidence and later improve the classification accuracy. Raoof (2020) [11] discusses the importance of early detection, prognosis and diagnosis in lung cancer, which continues. Various ML algorithms (Naive Bayes, support vector machine (SVM), logistic regression, and ANN) are reviewed with their application in diagnosis and research of lung cancer. Mohammadi (2019) [12] explained how medical information growing more and more speedy and complicated impedes effective use of physicians and increases the chance of human error in

interpreting data. Radiomics can process big data images to achieve this. R. P.R. (2019) [13] shows the incidence of lung cancer is increasing, it is necessary to investigate lung cancer which has a serious risk of death. In this work, we evaluated different classification methods: Naive Bayes, support vector machine (SVM), decision tree, and logistic regression to see if they could predict lung cancer. Z. Li et al. (2021) [14] have solved the important problem of examining pathological conditions of cancer cells suitable for curing patients. Here, they have launched the ACDC@LungHP campaign, that evaluates. The dataset for this challenge consists of 150 reference images and 50 test images. S. H. Hawkins et al. (2014) [15] In order to test the feasibility of using CT image features to predict outcome of non-small cell lung cancer, analysing cases with adenocarcinoma subtype. Extracting 3D features from CT scans by radiography, they then used that to create a classifier to predict survival. N. S. Nadkarni and S. Borkar (2019) [16] presents lung cancer diagnosis from CT images is proposed, which solves interpretation related concerns that can contribute to delayed, erroneous diagnosis. They preprocess images with a median filter and mapping onto a section of the lung of interest using mathematical morphology. F. Taher and R. Sammouda (2011) [17] The challenge of early diagnosis of lung cancer is addressed by two segmentation methods: HNN and FCM clustering algorithm. The research here is segmentation of color images in sputum as previous manual analysis is time consuming and is often erroneous to diagnosis. D. P. Kaucha (2017) [18] presents the usage of the support vector machine (SVM) products in biomedical image processing and their use to improve early detection of lung cancer were presented. They use data mining coupled with image processing technology to enhance accuracy, sensitivity and specificity of lung cancer diagnosis. X. Wang et al. (2020) [19] proposed to solve the difficulty of histopathology image classification, all lung cancer images are analyzed by an unsupervised method. As diagnosis is good and accurate for good patient treatment, but at present computer aided diagnosis is less used in diseases as there is less pixel annotation and tumor patterns in large scale images, they say. J. Alam, S. Alam, and A. Hossan [20] proposed a multilevel lung cancer diagnosis and prediction algorithm based on multivariate SVM classifier is presented. The authors highlight the importance of early diagnosis to raise patient survival and question whether we still need additional help in fulfilling accurate diagnostics of breast cancer. M. Jamshidi et al. (2020) [21] examine the huge pressures placed on global health system by the Covid-19 pandemic and the need for an effective response. [22] proposed a DL based weak diagnosis framework for rapid and accurate diagnosis of COVID-19 using chest CT images. Timely recognition for isolation and effective treatment is important and this study highlights this. To infer the outcome a 3D deep neural network is then applied to proposed method to process previously trained UNet model that segment lung in 3D CT volume. Y. Pathak (2021) [23] introduced a DBM network integrated with a so-called hybrid density network (HDN) for the classification of COVID-19 patients based on chest computed tomography (CT) images. In particular, the outbreak of novel coronavirus pneumonia (COVID 19) in December of 2019 evidenced the need for better diagnostic tools, which are more sensitive than CT imaging, but RT PCR is still important. S. A. -F. Sayed (2021) [24] Instead, focus on developing predictive models to determine how bad patients are going to be with COVID-19, especially if they have X-rays indicating it way early before a person is sick. With the high mortality rate of SARS-CoV-2, the goal of this research is to generate timely, accurate intelligence so physicians can make decisions. M. J. Horry et al. (2020) [25] checks out how early detection of COVID-19 using a series of imaging modalities, including X-ray, ultrasound and CT scan, is revolutionizing science. Our goal in these studies is to help non-invasive doctors with best deep learning images that may assist in diagnosing COVID-19.

3. PROPOSED WORK

In the proposed work, we have attempted to evaluate and compare the depth learning (CNN, VGG) to conventional machine learning methods (logistic regression, SVM, decision trees, Xgboost, AdaBoost). ResNet 19, ResNet 50 and ResNet 101 are designed to diagnosis of Breast cancer, lung cancer and COVID19 which are target diseases. For diagnosis, we will use denoising, normalization and enhancement of real emotional models on medical images. Each model will be trained and tested on these processed images and these images will then be processed to evaluate the classification. So we will evaluate each algorithm to determine which one metrees best regarding each key metric e.g precision, recall, F1 score, and computational efficiency. Once, we utilize deep learning models in a combo, then if it will work or not, if we can yield much better insights and increased accuracy of diagnosis.

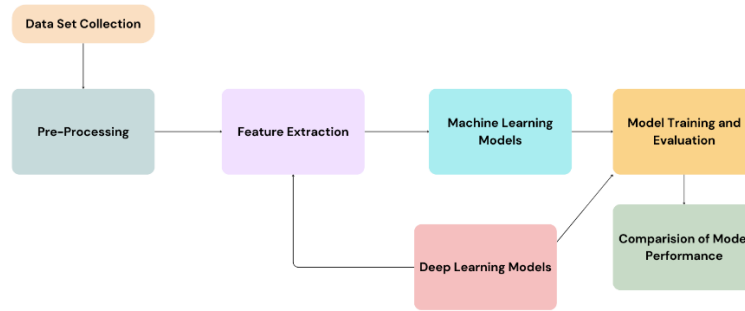


Figure 3.1: Proposed Architecture

3.1 Breast Cancer:

3.1.1 Dataset Description: Clinical images of breast cancer cases used are divided into two groups: benign and malignant. To perform model training, we have divided the dataset into training sets and test sets. The trained images and test images are separated into two group, i.e. there are a total of 8000 training images, 2000 test images.

- Training Set:
 - Breast Benign Images: 4,000 images
 - Breast Malignant Images: 4,000 images
 - Therefore, you will want to keep 20% of the training data subset (1,600 images) aside for performing model performance evaluation during the training phase.
- Testing Set:
 - Breast Benign Images: 1,000 images
 - Breast Malignant Images: 1,000 images

3.1.2 Pre-processing and Feature Extraction:

In this study, original breast cancer data were cleaned to make sure the data is in good condition for ml and dl models. The final process needs a pre-processing step since it helps the model to perform better by modeling the data and making the approaching image consistent (input image).

- **Image Rescaling:** All images in the dataset are rescaled to normalize pixel values to the range [0, 1]. This is accomplished by the equation:

$$I'_{i,j} = \frac{I_{i,j}}{255} \quad (1)$$

The parameters of the above refer to the image in the image, i and j are image points in the image, I is the initial pixel value and I' is the rescaled pixel value. This helps models connect faster during training by limiting the effect of different lighting conditions in different images thus normalizing pixel value.

- **Image Resizing:** The image is resized to 150x150 pixels for each image. This change may indicate:

$$I' = f(I, \text{target_size}) \quad (2)$$

More specifically for i = original image i' = resized image ff = resize function (e.g. bilinear or nearest neighbour) target_size = target size (150x150 pixels).

- **Data Splitting:** The input is split into training and validation sets to prevent overfitting. This can be defined as:

$$D_{train} = D[0: 0.8N], \quad D_{val} = D[0.8N: N] \quad (3)$$

- **Data Shuffling:** Images are shuffled to avoid model learning patterns from order of images, but this is something that it gets harder to control while evaluating on a test set. To accurately assess the model's performance, the parameters with which it is validated and tested remain unchanged.
- **Batch Processing:** The data is processed in batches of 32 images (set by the batch size parameter), which can be organized into batches as follows:

$$B_k = D[k \cdot B : (k + 1) \cdot B] \quad (4)$$

B_k is the k th batch, k is the batch index, and $B = 32$ the batch size. It speeds up training and reduces memory.

- **Class Mode (One-Hot Encoding):** We set the class mode to be categorical, i.e. label one-hot encode. This can be expressed as:

$$y'_i = \begin{cases} 1 & \text{if } y_i = j \\ 0 & \text{otherwise} \end{cases} \quad (5)$$

3.1.3 Machine Learning Model Architecture

a. Logistic Regression: Logistic regression as a widely used method of binary function classification can extend to many situations including predicting different type of breast cancer with image data.

The output of the linear combination z of input x will be denoted as:

$$x = \text{Flatten}(\text{input}) \quad (6)$$

SoftMax function:

$$p_i = \frac{e^{z_i}}{\sum_{j=1}^K e^{z_j}} \quad (7)$$

b. SVM (Support Vector Machine): A powerful new approach to breast cancer classification surface data can be provided by building an SVM-like neural network model.

Hinge Loss Function:

$$L(y_{\text{true}}, y_{\text{pred}}) = \frac{1}{N} \sum_{i=1}^N \max(0, 1 - y_{\text{true}}^i \cdot y_{\text{pred}}^i)$$

c. Decision Tree: Good diagnosis and planning for treatment is dependent on classification of breast cancer. ML techniques on neural networks devised to analyse decision trees are used to characterize breast cancer types from tissue test papers.

Custom Loss function:

$$L(y_{\text{true}}, y_{\text{pred}}) = \sum_{i=1}^N (y_{\text{true}}^i - y_{\text{pred}}^i)^2 \quad (9)$$

d. Navie Bayes: Early detection and planning for breast cancer requires classification. ML algorithms, particularly neural networks that replicate the behavior of Naive Bayes classifiers, are used to robustly categorize breast cancer types making use of image data.

3.1.4 Deep Learning Model Architecture

a. CNN-1: Development of accurate diagnosis and treatment strategies of breast cancer cells requires classification. Image classification with images classification is a common issue of applying CNN is used in classifying the mammogram as benign or malignant.

Max Pooling Operations:

$$y = \max(x) \quad (\text{Pooling operation}) \quad (10)$$

b. VGG-16: Advantages of this system are security and automation. The VGG 16 is a pre trained convolutional neural network (CNN) that has been known to achieve best results in image classification. In this, we use VGG 16 architecture to classify the cancer images as benign or malignant.

Global Average Pooling:

$$x = \frac{1}{H \times W} \sum_{i=1}^H \sum_{j=1}^W f_{ij} \quad (11)$$

c. VGG-19: Deep learning has become an important tool for diagnosis: classification of breast cancer. For this application, we use a VGG-19 architecture, an advanced convolutional neural network (CNN) that has proved successful in image classification tasks. This classification is based on imaging. These criteria help classify breast cancer images as benign or malignant.

Dense Layer Activation:

$$z = \text{ReLU}(Wx + b) \quad (12)$$

d. ResNet-50: Breast cancer cell classification is an important clinical task. Deep learning, and specifically neural networks (CNNs), has improved the detection and classification of breast cancer using image data. Here, we employ deep CNN Resnet 50 to classify breast cancer images as benign or malignant. Residual Network (ResNet)-50 is a widely used CNN architecture that is greatly performed and deep. It has 50 layers and solves the incompleteness problem by introducing the concept of connectivity between parts that may help deeper communication.

Fully Connected Layers and Dropouts:

$$z = \text{ReLU}Wx_{\text{GP}+b} \quad (13)$$

Finally, we show the nonlinear connectivity after the ReLU activation function applied to the GAP layer after a thick layer with 256 neurons.

e. ResNet-101: Breast cancer is the most common form of malignancy globally, and early diagnosis is the best approach to increasing patient survival. We observe that machine learning techniques, in particular deep learning, performed well on image-based breast classification. Here, to classify breast cancer images as benign or malignant groups, we are using a ResNet-101 model.

$$y = \mathcal{F}(x, \{W_i\}) + x \quad (14)$$

Where,

- x is the input,
- $\mathcal{F}(x, \{W_i\})$ is the residual function representing a series of convolutional, batch normalization, and activation layers,
- Y is the output of the residual block.

f. CNN-2: CNN-2 is an enhanced version of CNN-1 that includes additional regularization techniques such as Dropout layers. These changes help to reduce overfitting, especially when dealing with limited data, as breast cancer classification.

$$(I * K)(x, y) = \sum_i \sum_j I(x - i, y - j) \cdot K(i, j) \quad (15)$$

Model: "sequential_4"

Layer (type)	Output Shape	Param #
conv2d (Conv2D)	(None, 148, 148, 32)	896
max_pooling2d (MaxPooling2D)	(None, 74, 74, 32)	0
dropout (Dropout)	(None, 74, 74, 32)	0
conv2d_1 (Conv2D)	(None, 74, 74, 64)	18,496
max_pooling2d_1 (MaxPooling2D)	(None, 37, 37, 64)	0
dropout_1 (Dropout)	(None, 37, 37, 64)	0
conv2d_2 (Conv2D)	(None, 37, 37, 128)	73,856
max_pooling2d_2 (MaxPooling2D)	(None, 18, 18, 128)	0
dropout_2 (Dropout)	(None, 18, 18, 128)	0
flatten_4 (Flatten)	(None, 41472)	0
dense_4 (Dense)	(None, 256)	10,617,088
dropout_3 (Dropout)	(None, 256)	0
dense_5 (Dense)	(None, 2)	514

Total params: 10,710,850 (40.86 MB)
Trainable params: 10,710,850 (40.86 MB)
Non-trainable params: 0 (0.00 B)

Fig 3.1.4.1 CNN-2 Architecture for Breast cancer

3.1.5 Model Training and Evaluation

Breast cancer classification is a process of training and evaluating how learning machine learning algorithms work from data. The dataset is split initially into training, validation, and testing excerpts, wherein, the input set is used within the model to train the model, the validation set is used to tune hyper parameters and the testing set used to ascertain performance of the model. In contrast forward propagation predicts the outputs and loss function rates the gap between actual and predicted labels through training. It works back to adjust model weights such that loss minimization will increase accuracy.

3.1.6 Comparison of Model Performance

This is important to select the most effective algorithm for breast cancer classification. Once we have each model's performance, it can be the accuracy, precision, recall or F1 score, so we've got a quantitative way to compare them. Training time is also a major aspect, as more complicated models may achieve greater accuracy, but take a longer time to train, which would be impractical in clinical setting. We analyse overfitting by looking at training vs validation performance, this can help us find models which may not generalize to new data.

3.2 Lung Cancer:

3.2.1 Dataset Description:

This lung cancer classification project has used a dataset of images collected from some sources and are categorised into three different classes which signify the different types of lung cancer. Below is a summary of the dataset:

- Total Images: Training, validation, and testing sets with 12,000 images respectively.
 - Training Set:
 - 9600 images (80% for training and 20% for validation).
 - During training the model is validated on 2400 images.
 - Testing Set:
 - In the final model's performance evaluation using 3000 images.
- Classes:
 - Adenocarcinoma (lung_aca): An early lung cancer that develops within glandal tissue.
 - Bronchial Carcinoma (lung_bnt): A common type of lung cancer that starts in the bronchial tubes.

- Squamous Cell Carcinoma (lung_scc): Cancer that begins in the squamous cells that form the inside lining of the airways.

Each class has its subdirectory containing the images and it's pretty easy to load them using Keras's ImageDataGenerator.

3.2.2 Pre-processing and Feature Extraction:

Preparing data to train machine learning model (To Enable training models) is a crucial step and it is called preprocessing. In this project, the following steps were undertaken:

- Image Rescaling:
 - We rescale all images to uniform size of 150x150 pixels.
 - It also normalizes pixel values to 255 which, in practice, improves convergence during model training. dividing by 255, which improves convergence during model training.

$$I' = \frac{I}{255} \quad (16)$$

- Data Augmentation:
 - To enhance the diversity of the training dataset and reduce overfitting, data augmentation techniques are employed, including:
 - Rotation: Randomly rotating images in order to add variability.
 - Width and Height Shift: Simply 'randomly' translate images along the x and y axis.
 -
- Train-Validation Split:
 - While performing data augmentation the training dataset is divided into training data of 80% and the validation data of 20% through the validation split in ImageDataGenerator function. This affords an opportunity for performance assessment during training.

$$N_{\text{val}} = 0.2 \times N_{\text{train}} \quad (17)$$

$$N_{\text{train_final}} = 0.8 \times N_{\text{train}} \quad (18)$$

- Batch Processing:
 - Images are grouped in folders and the flow_from_directory loads them in batches which exempts them from time-consuming data loading process.. So, batch size is chosen to be 32 – this way, the model gets reasonable portions of samples per updates step.
- Class Mode:
 - For multi-class classification, the class mode is set to 'categorical', allowing for SoftMax activation in the output layer of the model.

3.2.3 Machine Learning Model Architecture

a. Logistic Regression: This lung cancer classification by logistic regression model accepts images of 150x150x3 and 150x150x3 and redescribe them as vectors of 67,500 in size. The model then computes a weighted sum for the three classes adenocarcinoma, "BNT", squamous cell carcinoma.

$$L = -\sum_{c=1}^3 y_c \log(p_c) \quad (19)$$

b. SVM: The classification model for lung cancer based on SVM like model employs a neural network structure for SVM.

$$z_c = \sum_{i=1}^{67500} w_{i,c} x_i + b_c \quad (20)$$

c. Decision Tree: The lung for cancer classification model by using neural network structure a lot like the idea of decision tree with enhancement of capability of neural network.

$$L = \sum_{i=1}^n (y_i - z_i)^2 \quad (21)$$

d. Navie Bayes: The usage of Naive Bayes-like neural network for classification of lung cancer features employs a simple architecture that ape the probabilistic naiveness of Bayes' method.

$$\text{Test Loss} = L_{\text{test}} = - \sum_{c=1}^3 y_c^{\text{test}} \log(p_c^{\text{test}}) \quad (22)$$

3.2.4 Deep Learning Model Architecture

a. CNN-1: Other features CNN-1 model for lung cancer classification aims at identifying the probability distribution over multiple classes including adenocarcinoma, “BNT,” and squamous cell carcinoma from the lung images.

$$Z_{\text{dense}} = W_{\text{dense}} \cdot A_{\text{flat}} + b_{\text{dense}} \quad (23)$$

b. VGG-16: The VGG-16 model is a deep convolutional neural network architecture known for its depth and effective feature extraction capabilities.

c. VGG-19: Lung cancer images are classified using the VGG-19 model. The architecture of this kind of system is most suited for feature extraction and classification. Training, evaluating, and metrics calculation of the model are performed, and some important values are calculated.

d. ResNet-50: The results obtained with the ResNet-50 model are used for the classification of lung cancer images. Its architecture takes advantage of the residual connections in training of deeper networks. Model training is done followed by model evaluation and different calculations are performed to check the competency of the model.

e. ResNet-101: analysis of ResNet-101 model is that the preprocessing and data augmentation used to prepare data for learning significantly affect the final model. The rotation, zoom, and horizontal flip techniques can be used to generate more data to train on and the model generalizes better than when all the data is augmented thus preventing overfitting.

f. CNN-2: The CNN_1 model serves as a base setup that serves for the optimized and enhanced version of CNN_1, denoted as CNN_2, which relies on the same architectural basis by incorporating a variety of advanced technologies to yield better performance in tasks of lung cancer classification. A deeper CNN-2 with additional convolutional and pooling layers is employed by CNN-2, which is capable of capturing more complex cues, and learn hierarchical patterns in the images. It also batch normalizes the outputs of each convolutional layer (i.e. normalizes the inputs), to speed up training and make the network stable.

Model: "sequential_14"

Layer (type)	Output Shape	Param #
conv2d (Conv2D)	(None, 148, 148, 32)	896
max_pooling2d (MaxPooling2D)	(None, 74, 74, 32)	0
conv2d_1 (Conv2D)	(None, 72, 72, 64)	18,496
max_pooling2d_1 (MaxPooling2D)	(None, 36, 36, 64)	0
conv2d_2 (Conv2D)	(None, 34, 34, 128)	73,856
max_pooling2d_2 (MaxPooling2D)	(None, 17, 17, 128)	0
Flatten (Flatten)	(None, 36992)	0
dense_36 (Dense)	(None, 128)	4,735,104
dense_37 (Dense)	(None, 2)	258

Total params: 4,828,610 (18.42 MB)
 Trainable params: 4,828,610 (18.42 MB)
 Non-trainable params: 0 (0.00 B)

Fig 3.2.4.1 CNN-2 Architecture for Lung Cancer

3.2.5 Model Training and Evaluation

A dataset of chest X ray images was used to train and evaluate different machine learning models in the search of an effective lung cancer detection. In this case, we performed a training-validation split

to keep track of how well the model is performing and to not overfit. In addition to Logistic Regression, SVM, Decision Trees, Naive Bayes, CNN-1, ResNet-50, ResNet-101, etc. as each model.

3.2.6 Comparison of Model Performance

Results showed that CNN architectures (CNN-1, CNN-2; VGG-16, VGG-19; ResNet-50, ResNet-101) exceeded the accuracy and robustness to over fitting of conventional machine learning models. Batch normalization, dropout, and residual connections — implemented as enhancements — improved generalization and better behaved when faced with complex features from the data. Generally, the findings highlight the effectiveness of deep learning approach both in supporting medical image analysis and for potentially critical applications, such as lung cancer detection.

3.3 Covid-19:

3.3.1 Dataset Description:

The dataset used for COVID-19 detection comprises two primary categories of CT images: Positive and non-positive (healthy) for COVID. It has 4,000 images of CT scans of each type making a total of 8,000 images. The clinical images are COVID and non-COVID, which are supplemented from several clinical setting to have a diverse representation of the pulse of the disease in the lungs. The dataset is balanced, so it has same number of samples from both classes to train robust machine learning model. Size of each image is 224x224 pixels and can be used to feed the pre-trained models expecting a constant size.

3.3.2 Pre-processing and Feature Extraction:

Before training the models, the dataset is pre processed to some extent thereby transforming the images to serve a better quality and bring about a better extraction of features. OpenCV reads the images and converts them to the RGB representation, then resizes to 224 x 224 pixels so that they match input size for deep learning models. So when used for training this helps in speeding up convergence by dividing each pixel value by 255 so that it normalizes the values to range [0, 1] Furthermore, the dataset was further split to train and test set, keeping 20% of the images aside for the model testing..

3.3.3 Machine Learning Model Architecture

a. Logistic Regression: Simple and interpretable model, logistic regression is used as a baseline. A logistic function is used to calculate the probability of the input being positive (COVID positive) class.

$$P(y = 1|X) = \frac{1}{1+e^{-\beta^T X}} \quad (24)$$

b. SVM: It uses SVM because it finds a hyperplane in high dimensional spaces that best separates the classes. The model itself is trained on the CT images with the goal to maximize the margin of binary classification COVID or non-COVID.

c. Decision tree: A nonlinear approach to classification is provided by implementing a Decision Tree classifier. It makes splits on the base feature values to form the tree like structure which helps to make decisions.

d. Xg-Boost: It is leaning on XGBoost (Extreme Gradient Boosting) on its efficiency and effectiveness of dealing with structured data. It consists of a sequential construction of multiple weak learners (decision trees) which build an ensemble learning in an optimizing scheme of errors made so far by the previously equipped trees.

e. Ada-Boost: We have also included the strong ensemble method AdaBoost (Adaptive boosting). It tries to find misclassified samples of the previous iterations and combines these filters to produce a strong prediction model.

3.3.4 Deep Learning Model Architecture

a. CNN-1: In reality, the simple CNN-1 model we present in this study is actually a very simple model comprised of the main elements of convolutional neural networks, as a base. Each followed with ReLU activation brings non linearity to the model so that it can learn complicated patterns of CT scan images.

b. VGG-16: VGG-16 is a well known deep learning architecture that is known for both depth and effectiveness in the image classification tasks. This is a model of 16 layers with learnable parameters, 13 convolutional layers, 3 fully connected layers. After each block of convolutional layers we apply a set of max pooling layers that systematically reduces the spatial dimension of an input image keeping only the important features.

c. VGG-19: VGG-19 has 19 layers with learnable parameters, so that's one more than this — yay, one extra convolutional layer! This offers an additional depth, allowing the model to absorb a wealth of more complex properties of CT image input. As with VGG-16, VGG-19 also adheres to the same design philosophy, but exchanges the size of the convolutional filters from $3 \times 3 \times 3$ to $3 \times 3 \times 3$, $2 \times 2 \times 2$ max pooling layers (which may get better for some tasks).

d. ResNet-50: In this work, we present a path breaking deep learning with ResNet-50, a novel residual learning framework. In this architecture, I have 50 layers and employ skip connections which help the gradient flow in both directions in the back propagation that overcomes vanishing gradient problem suffered by the deep networks.

e. ResNet-100: Using the same principles that were used in ResNet-50 the ResNet-101 is built with 101 layer in order to increase the learn complex patterns input data outputs. It is similar to its predecessor ResNet-101 that uses residual connections, so that the information loss in training deep networks does not occur.

f. CNN-2: CNN-2 is an optimized version of CNN-1 architecture, without constraints seen in the previous experiments which are added to the CNN-1 architecture or are drawn from the insights of the previous experiments. For example, this model is a little bit more complex model in its architecture, because it has more based convolutional layer and uses better pooling strategy to better extract feature.

3.3.5 Model Training and Evaluation

In medical as distinguishing COVID-19 from CT scans, robust machine learning systems rely heavily on model training and evaluation. For this study, the prepared dataset we had a balanced mix of images from COVID-19 and non COVID-19 and each deep learning model (CNN-1, VGG-16, VGG-19, ResNet-50, ResNet-101, CNN-2) was trained with this database. The training process was to split up the given dataset into training and testing and validate subsets, so that our models learn the right stuff but will also be tested on the unseen data.

3.3.6 Comparison of Model Performance

Finally, the performance of the proposed architecture is compared to other models in order to identify the best model for classifying COVID-19 cases based in CT scans. For that we have seen overall performance of each model using different metrics of performance. Key metrics included accuracy, precision/true positive rate or recall and F1 score and area under the ROC curve (AUC). We checked these metrics on each model and on each model, the results were markedly different. For instance, the more traditional CNN architectures (e.g., CNN-1), had reasonable accuracy, however more sophisticated architectures, i.e. VGG-19 and ResNet-101, have better accuracy and generalization towards unseen data. But in this case, with higher recall, VGG-19 was deeper and hence better at extracting high level relevant features, particularly for the minority class. ResNet-50 and ResNet-101

trained on deeper networks without the performance degradation, and adapting residual connections with CT images achieved impressive classification of the CT images as the CT images themselves.

4. EVALUATION AND RESULTS:

In the evaluation and results section, all the findings are synthesized from which machine learning and deep learning models extrapolated towards detecting breast cancer, lung cancer, and COVID-19. A multitude of metrics were used to pathetically test the performance of each model, such as accuracy, precision, recall, F1-score, and area under the receiver operating characteristic curve (AUC-ROC). These metrics gave me a complete picture of the ability of the models to classify whether a case was malignant or not — for breast cancer, to differentiate between types of lung cancer, — and to classify whether a CT scan is positive for COVID or not.

4.1 Breast Cancer:

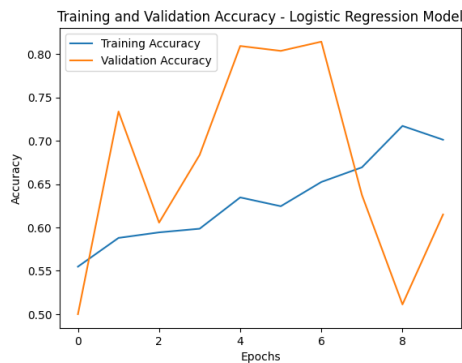


Fig 4.1.1 Logistic Regression Accuracy for Breast Cancer

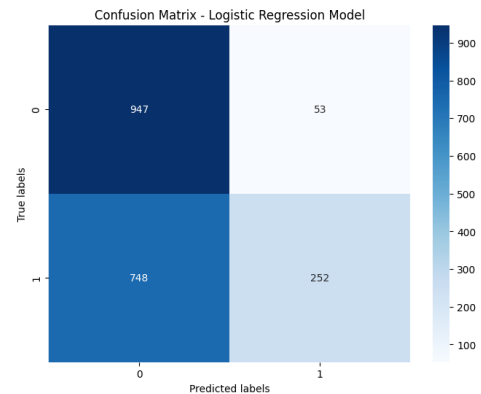


Fig 4.1.2 Logistic Regression Confusion matrix for Breast Cancer

Logistic Regression yielded outcome where the model had a training accuracy of 70% and a validation accuracy of 60% in the classification of breast cancer as shown in fig 4.1.1. The confusion matrix is depicted in the figure 4.1.2 below; the results show that class 0 was classified with high accuracy, the model yielded 947 true positive. However, evaluating all the results it was evident that the model was not so good when it came to class 1, given that it misclassified 748 as negatives or as being in the same class as 0.

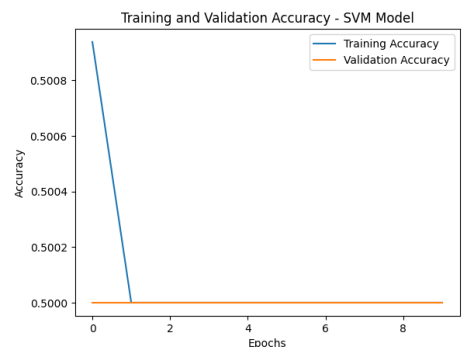


Fig 4.1.3 SVM accuracy for Breast Cancer.

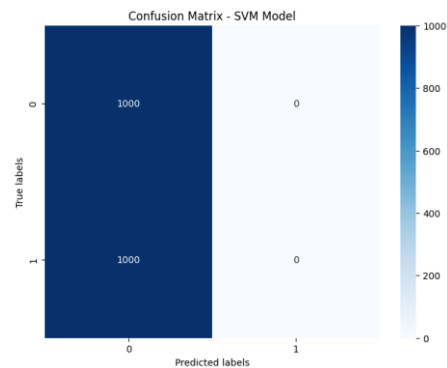


Fig 4.1.4 SVM Confusion Matrix for Breast Cancer.

The SVM model illustrating in Fig 4.1.3 performed 50% training accuracy and 50% validation accuracy in breast cancer classification. However, based on the confusion matrix shown as in Fig 4.1.4 below, the model has the following major concerns. It sets all instances into the class 0, marking all of them as true positive, although 1000 of them are actually right, while misclassifying 1000 instances of class 1 into class 0, making them false positive. This raises questions about the quality of class balance or signals

that may be mixed within a class and require pre-processing to correct in order for the model to be effective.

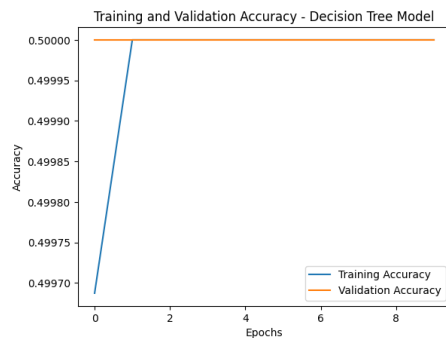


Fig 4.1.5 Decision Tree Accuracy for Breast Cancer.

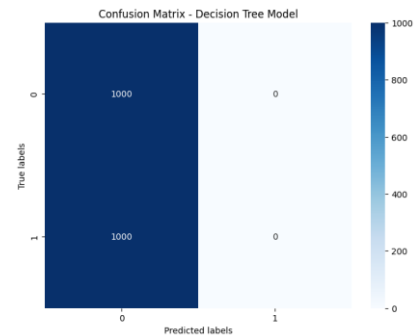


Fig 4.1.6 Decision Tree Confusion Matrix for Breast Cancer.

From Fig 4.1.5 below illustrate the performance of decision tree model, Where the training and validation accuracy remains constant at 50% over epochs proving that the model is not capable of over learning but at the same it is not learning effectively at all. This is further demonstrated in the confusion matrix in fig 4.1.6 where the model only predicts all instances as class 0, 1000 samples of which are correctly classified from class 0 while the same model completely misses class 1 with 1000 false negatives. This shows that at most times, there are extreme cases of class imbalance or model bias that require resolution.

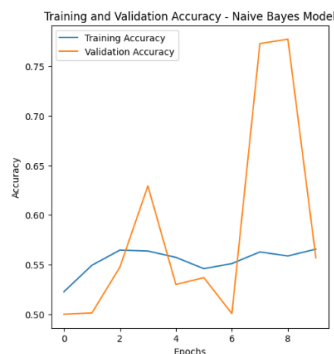


Fig 4.1.7 Naïve Bayes Accuracy for Breast Cancer.

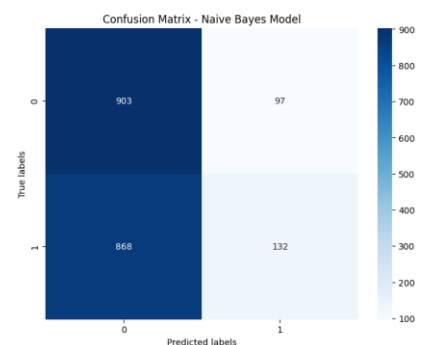


Fig 4.1.8 Naïve Bayes Confusion Matrix for Breast Cancer.

For breast cancer classification, a Naive Bayes model that is illustrated in Fig 4.1.7 provided the training accuracy of 57% as well as the validation accuracy of 54%. However, as shown in the confusion matrix in Fig 4.1.8, the model identifies only class 0 with 903 instances correctly classified in class 0 though it does not recognize at all class 1 with 868 instances misclassified as negative. These results emphasize high difficulties in managing class 1 possibly owing to distribution imbalance or some shortcomings in the model so appropriate ways must be sought to manage class 1.

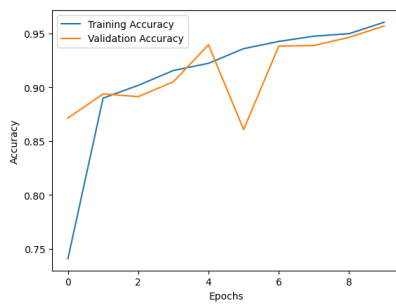


Fig 4.1.9 Optimized CNN Accuracy for Breast Cancer.

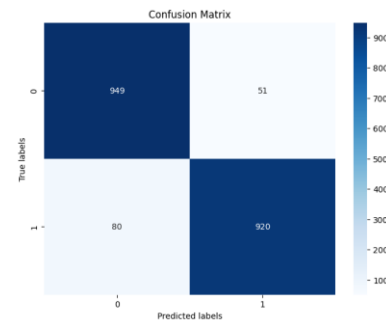


Fig 4.1.10 Optimized CNN Confusion Matrix for Breast Cance

It is obvious a sufficient level of learning from Fig 4.1.9 highlighting the training and validation accuracy of CNN model. It achieves a training accuracy of 0.75 when trained for one epoch and increases to 0.95 at nine epochs. Again, the training and validation accuracy trace similar paths, though the accuracy falls away slightly at epoch 4, possibly due to overfitting or, more likely, variation in the training data, before approaching the near-rentch training accuracy of 0.95 in the later epochs. Shown in the confusion matrix in Fig 4.1.10 is the models high performance and high true negatives of 949 and true positives of 920. However, the model commits 51 false positives and 80 false negatives for the negatives and positives respectively that can be improved upon to decrease the misclassification errors.

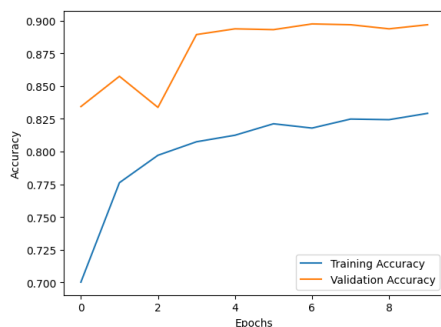


Fig 4.1.11 VGG-16 Accuracy for Breast Cancer.

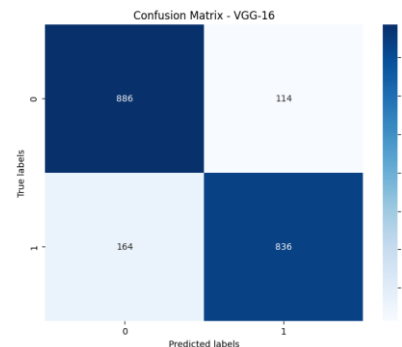


Fig 4.1.12 VGG-16 Confusion Matrix for Breast Cancer.

Hence, the VGG16 model has impressive simulation capability as depicted in fig 4.1.11 where VGG16 model training accuracy rises from 70% to 80% levels as shown below. The validation accuracy stands higher and stays within the range of 87% to 90%, which means good generalization of the calculated model without the sign of overfitting. This is also highlighted by the confusion matrix in fig 4.1.12 consisting of 886TN, 836TP, 114FP, 164FN. The show that the classification performance is quite good, as in most cases correct classification is achieved; however, there is certain room for improvement in terms of false classification.

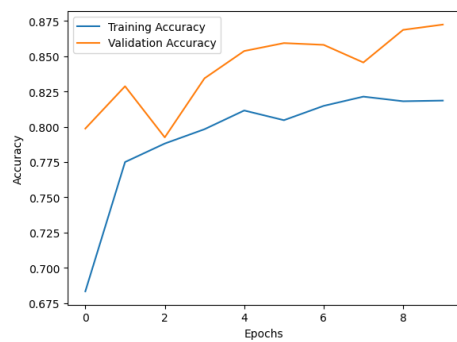


Fig 4.1.13 VGG-19 Accuracy for Breast Cancer.

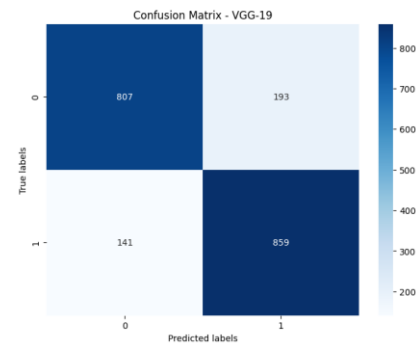


Fig 4.1.14 VGG-19 Confusion Matrix for Breast Cancer.

The VGG19 model shown in fig 4.1.13 has training accuracy starting from 70% to 80% while validation accuracy from 80% to 87%. This suggests good level of generalization with slight over training in the model. The confusion matrix of Fig.4.1.14 further supports reliable performance with 807 correct predictions for class 0 and 859 for class 1. But the model wrongly predicts 193 samples of class 0 as class 1 and 141 samples of class 1 as class 0. It can be clearly seen that it has adequately classified most of the data, but there are some mistakes that can tell us where more improvement is needed.

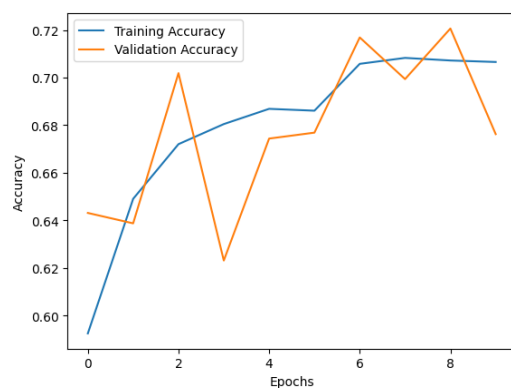


Fig 4.1.15 ResNet-50 Confusion Matrix for Breast Cancer.

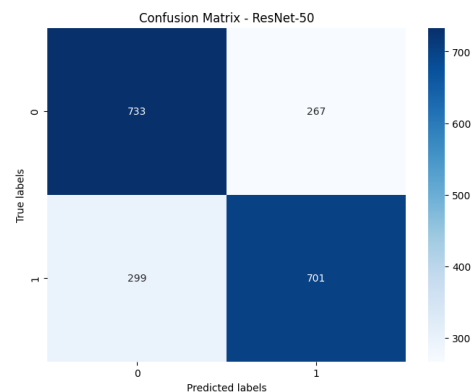


Fig 4.1.16 ResNet-50 Confusion Matrix for Breast Cancer.

As seen earlier in Fig 4.1.15 the ResNet-50 model gives training accuracy variability in between 60 – 70 % and validation accuracy variability between 64 – 68 % . This implies that there is a scope of even better model generalization given the observed small margin of difference between the training and validation loss. Classes 0 and 1 in confusion matrix of Fig 4.1.16 represent the samples that are predicted by the model while class 1 in the actual class: The specific details include 753 instances of class 0 samples predicted correctly and 299 instances of class 1 samples in actual class but predicted as class 0. This implies that in the optimization of model for classification, class 1 may be learn in lesser degree compared with class 0, and this may provide insight into which aspect of class 1 the model needs help in handling.

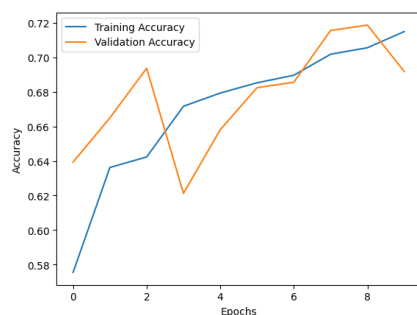


Fig 4.1.17 ResNet-101 Accuracy for Breast Cancer.

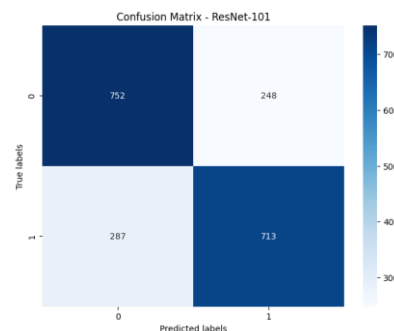


Fig 4.1.18 ResNet-101 Confusion Matrix for Breast Cancer.

For training accuracy, ResNet-101 model as presented in Fig 4.1.17 above has a fluctuation of between 58% and 72%, on the other hand, the validation accuracy has a range of between 64%- 69%. This shows continued enhancement but also points to the fluctuation in validation result: more scopes for better generalization needed. As can be seen from Fig 4.1.18 confusion matrix, 287 samples of class 1 can be classified correctly, but 752 samples of class 0 are misclassified. However, this seems to be a tiny improvement in performance for class 1 while the model is not effective in the prediction of class 1 instances at all, and needs more fine-tuning.

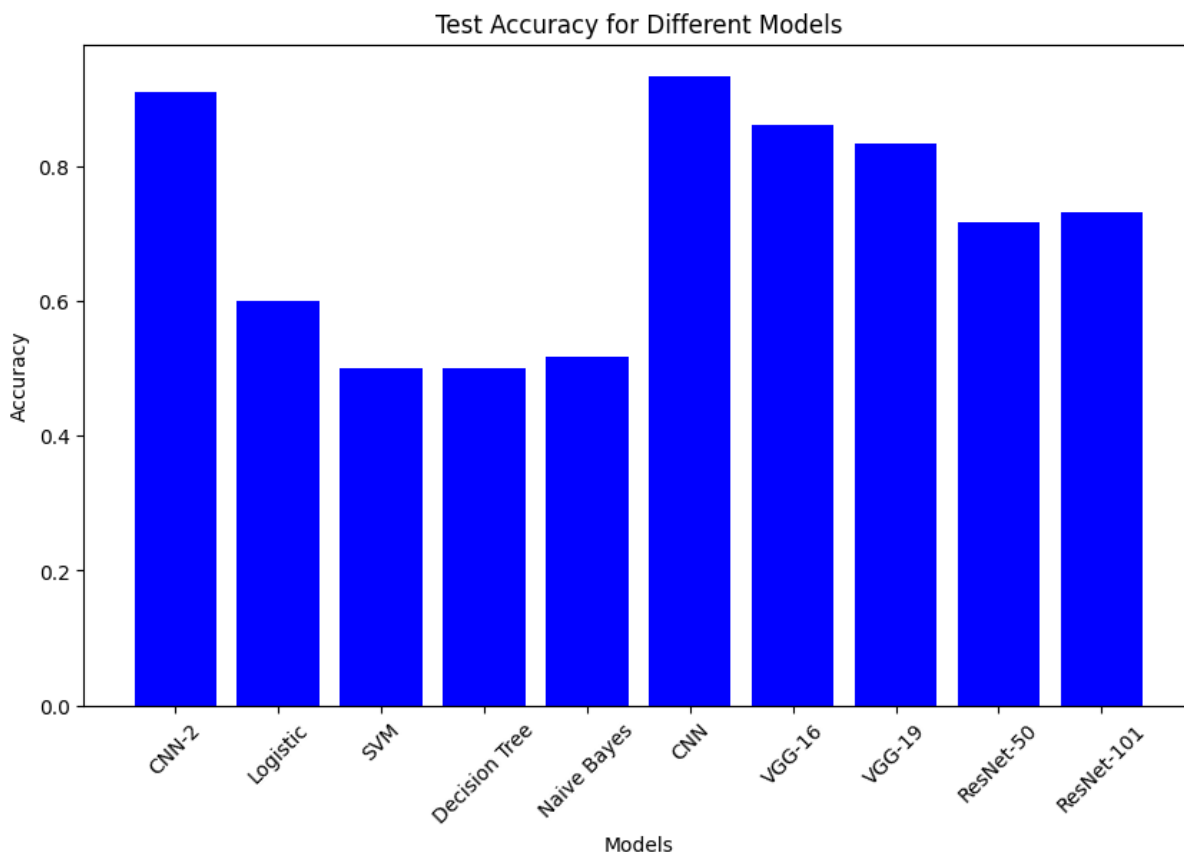


Fig 4.1.26 Bar Graph which shows differences between all models for Breast Cancer

Table 4.1.1: Differences Between All Machine Learning and Deep Learning Models

SNO	Model Name	Accuracy	Loss	Precision	Recall	F1-Score
1	Logistic Regression	59.9%	45.06%	0 – 56% 1 – 83%	0 – 0.95 1 – 0.25	0 – 0.70 1 – 0.39
2	SVM	50%	50%	0 – 50% 1 – 50%	0 – 1.00 1 – 0.00	0 – 0.67 1 – 0.00
3	Decision Tree	50%	100%	0 – 50% 1 – 50%	0 – 1.00 1 – 0.00	0 – 0.67 1 – 0.00
4	Naïve Bayes	51.74%	35.39%	0 – 51% 1 – 58%	0 – 0.90 1 – 0.13	0 – 0.65 1 – 0.21
5	CNN - 1	90.95%	27.70%	0 – 89% 1 – 91%	0 – 0.91 1 – 0.88	0 – 0.90 1 – 0.89
6	VGG-16	86.10%	35.71%	0 – 84% 1 – 88%	0 – 0.89 1 – 0.84	0 – 0.86 1 – 0.86
7	VGG-19	83.30%	37.90%	0 – 85% 1 – 82%	0 – 0.85 1 – 0.86	0 – 0.83 1 – 0.84
8	ResNet-50	71.70%	57.90%	0 – 71% 1 – 72%	0 – 0.73 1 – 0.70	0 – 0.72 1 – 0.71
9	ResNet-100	73.32%	55.52%	0 – 72% 1 – 74%	0 – 0.75 1 – 0.71	0 – 0.74 1 – 0.73
10	CNN - 2	93.44%	16.44%	0 – 92% 1 – 95%	0 – 0.95 1 – 0.92	0 – 0.94 1 – 0.93

4.2 Lung Cancer:



Fig 4.2.1. Logistic Regression Accuracy for Lung Cancer.



Fig 4.2.2 Logistic Regression Confusion matrix for Lung Cancer.

As for the Logistic Regression model for breast cancer shown in Fig 4.2.1, it gains 70% accuracy in training set and 60% accuracy in the validation set. When comparing the results for lung cancer, the training accuracy floats between 68 and 77 % while the validation accuracy drops slightly between 76 and 75 % illustrating reasonably stable performance. The confusion matrix given in Fig 4.2.2 reveal that true and false positives and true and false negatives respectively for class 1 are fairly good with 988; the lower values, indicating a lower number of misclassifications. But it performs worst in class 0 and class 2 which in fact sometimes wrongly classifies some samples from class 0 as of class 2 recommending possible enhancement on the handling of such classes.

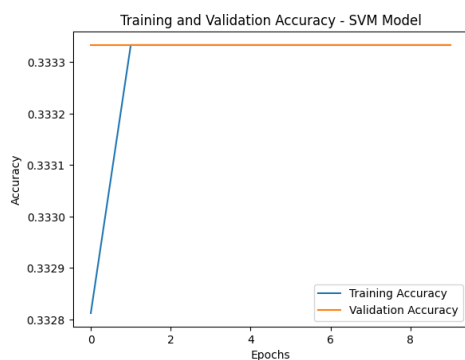


Fig 4.2.3 SVM accuracy for Lung Cancer.

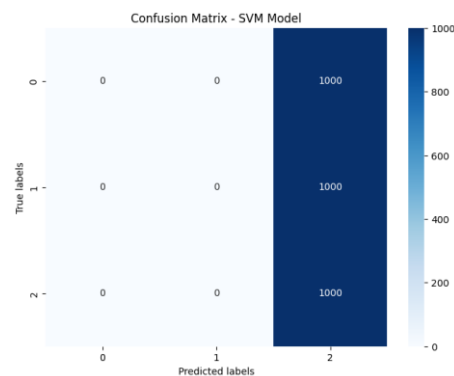


Fig 4.2.4 SVM Confusion Matrix for Lung Cancer.

Fig 4.2.3 demonstrates how poor, the model was in the training and validation scores were very low at 33% in the Support Vector Machine (SVM) model shown below. The other possibility is using a model that was not able to capture the data, or used too little training data or needed more fine tuning. We can see in Fig 4, all 1000 and the prediction true classes of class 2 gets misclassified to class 2 as well as the samples from classes 0, 1, 2 misclassified to class 2. So this could be because we are facing problems like data misbalanced or wrong choice of hyperparameters / features or no ability to separate multiple features correctly.

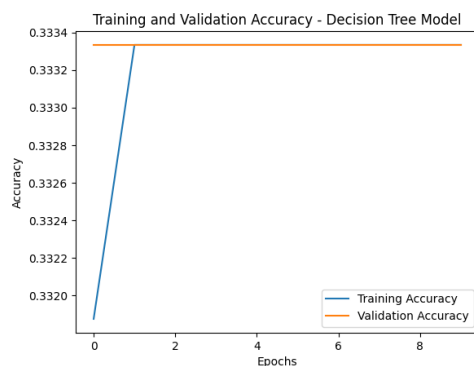


Fig 4.2.5 Decision Tree Accuracy for Lung Cancer

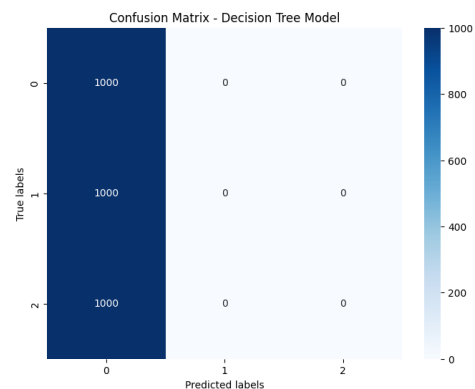


Fig 4.2.6 Decision Tree Confusion Matrix for Lung Cancer.

Fig 4.2.5 shows Decision Tree model; which achieved the same accuracy on training and validation which imply it is not learning properly. Therefore, it implies the need for being adjusted by hyper parameter tuning or feature engineering to enhance its performance. In Fig 4.2.6 we see that the model predicts all samples in classes 0, 1, and 2 to be class 0, and the model makes 1,000 predictions of class 0 for every true class in the confusion matrix. This means that our model is totally biased, probably wrongly trained, because the dataset is very imbalanced or it's just overfitted to a certain feature.

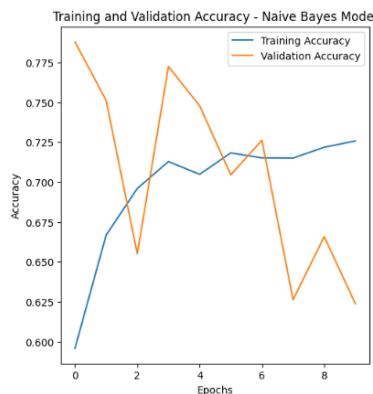


Fig 4.2.7 Naïve Bayes Accuracy for Lung Cancer.

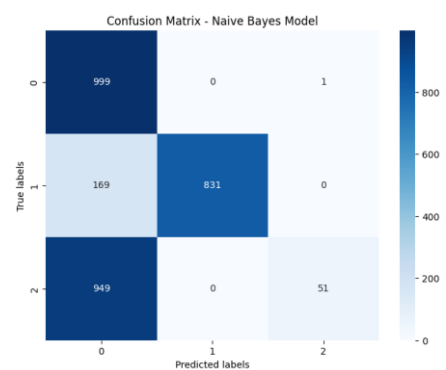


Fig 4.2.8 Naïve Bayes Confusion Matrix for Lung Cancer

As seen in Fig 4.2.7, the Naive Bayes model learns with reported values of training accuracy between around 60-72 percent and validation accuracy between 78-63 percent. When we first start running the model, it does relatively better on the validation set, i.e. it seems to not overfit too soon, but its performance drops as training goes on suggesting either overfitting or possibly instability in generalization. In Fig 4.2.8 the confusion matrix shows high accuracy for Class 0 (999 predictions correct) and Class 1 (831 predictions correct). But it works really badly for Class 2, (fuelling) the need to do better with Class 2.

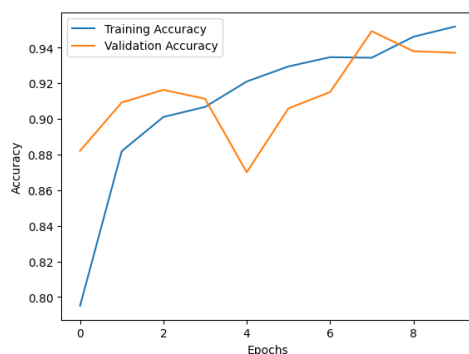


Fig 4.2.9 CNN-1 Accuracy for Lung Cancer.

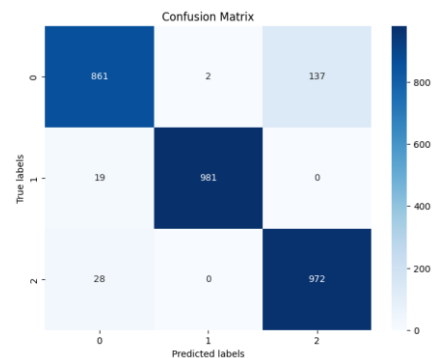


Fig 4.2.10 CNN-1 Confusion Matrix for Lung Cancer

Fig 4.2.9 shows the CNN model behaviour with training accuracy in the range of 80 to 95 percent and validation accuracy between 88 and 93 percent, suggesting good generalization, a small training validation gap for consistent performance. As can be seen from Fig 4.2.10 confusion matrix, all classes are totals with high accuracy with 88% accuracy for Class 0 and 137 classifies as Class 2 and 2 classifies as Class 1. The corrects predictions via Class 1 is 961 and misclassified 19 into Class 0, while Class 2 correctly predicts 972 and misclassified 28 into Class 0. While there is high overall accuracy of approximately 92%, most errors occur between Class 0 and Class 2, suggesting a need to refine in identifying these classes.

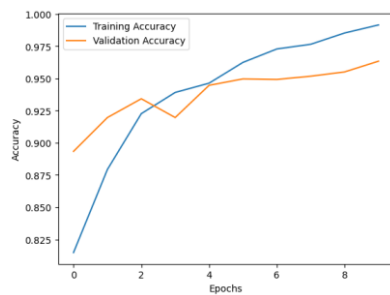


Fig 4.2.11 Optimized CNN Accuracy for Lung Cancer.

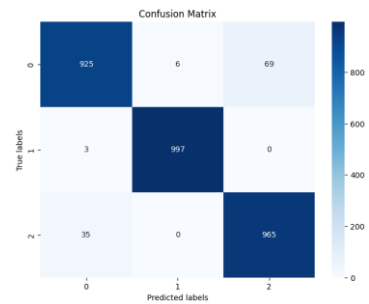


Fig 4.2.12 Optimized CNN Confusion Matrix for Lung Cancer.

Shown in Fig 4.2.11, the CNN model achieves ~ 99.5% training accuracy and about 97% validation accuracy by the last epoch, with validation accuracy stabilizing beyond epoch 5. This is strong generalization and very little overfitting as the gap between training and validation performance is very small. As shown in Fig 4.2.12, it clearly performs very well and produces 997 correct predictions for Class 1. Nevertheless, it turns out that most out of these misclassifications come from classes 0 and 2, where we have some instances in class 0 that get misclassified as class 2 and vice versa indicating that these classes should be better apart.

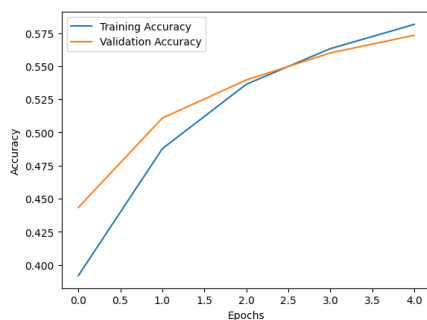


Fig 4.2.13 VGG-16 Accuracy for Lung Cancer.

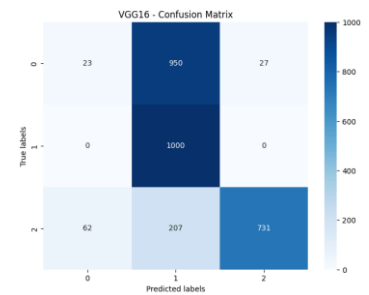


Fig 4.2.14 VGG-16 Confusion Matrix for Lung Cancer.

After comparing with our training and validation accuracy of 55%, we find that training and validation accuracy on the VGG-16 model shown in Fig 4.2.13 is 55% as well, which shows underperformance and suggests either additional tuning, additional data, or more sophisticated feature extraction to improve classification. The model correctly predicts in this form the correct output for 1,000 Class 1 cases, 950 of Class 0 (27 misclassified into Class 2), and 731 Class 2 (207 misclassified into class 1) as shown in Fig 4.2.14. Although the accuracy for Class 1 can be improved, it is still carrying the misclassification to Class 0 and Class 2, thus the overall performance should be improved.

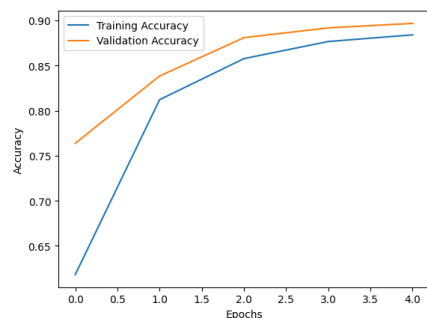


Fig 4.2.15 VGG-19 Accuracy for Lung Cancer.

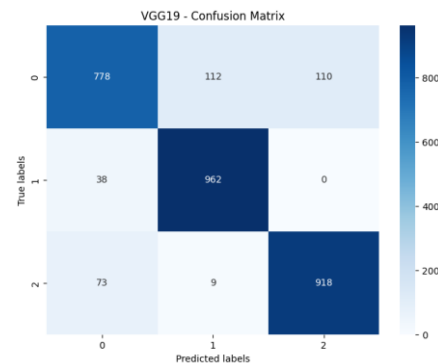


Fig 4.2.16 VGG-19 Confusion Matrix for Lung Cancer.

Train accuracy between 64% and 84% and validation accuracy between 76% and 90% is achieved with the VGG-19 model (Fig.4.2.15). Validation accuracy remains consistently higher implying that there is little overfitting and the learner is effective. In Fig 4.2.16, the confusion matrix shows which classes of the model were correctly predicted and which were not; the diagonal cells give rise to correct predictions (778 Class 0, 962 Class 1, 918 Class 2). However, the model gives the highest level of misclassification with the Class 1, and less with the Classes 0 and 2 which means there are some areas to improve.

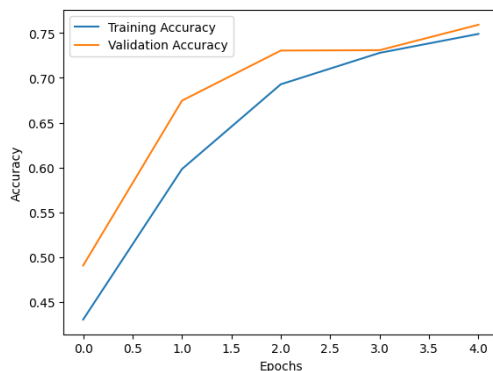


Fig 4.2.17 ResNet-50 Accuracy for Lung Cancer.

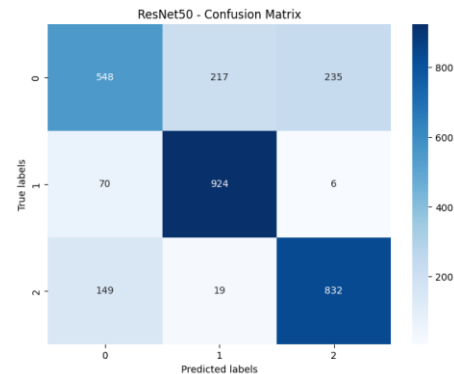


Fig 4.2.18 ResNet-50 Confusion Matrix for Lung Cancer.

As illustration in Fig 4.2.17, the training accuracy in the ResNet-50 model is 44% to 74%, validation is 50% to 75%, which means it has some improvement but not good enough generalization yet. Fig 4.2.18 is the confusion matrix which indicates that: 548 predicted correctly for Class 0; 924 for Class 1, and 832 for Class 2. Error rates are higher for Class 0 (217 misclassified as Class 1 and 235 as Class 2) and Class 2 (149 misclassified as Class 0). The model exhibits the best generalization for Class 1, and is extremely poor for Classes 0 and 2, implying that we have some work to do when dealing with these classes.

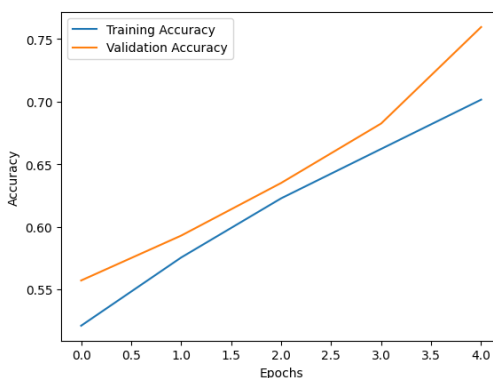


Fig 4.2.19 ResNet-101 Accuracy for Lung Cancer.

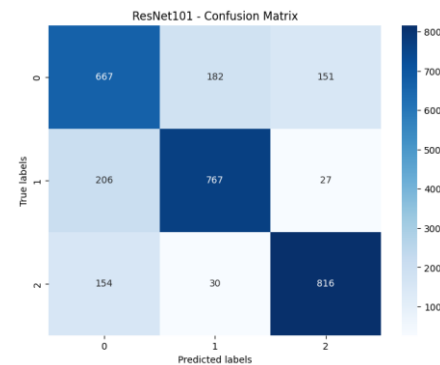


Fig 4.2.20 ResNet-101 Confusion Matrix for Lung Cancer.

Fig 4.2.19 shows the ResNet 101 model, which can train with an accuracy as low as 50% and less than 70%, and validates with an accuracy as low as 55% to approximately 76%. The validation accuracy continually improves, and is more stable than ResNet 50. From the confusion matrix in Fig 4.2.20 the model correctly predicts 667 of Class 0, 767 of Class 1 and 816 of Class 2. 206 Class 1's that should have been Classified as Class 0 and 154 Class 2's that should have been Classified as Class 0. The model does reasonably less than ResNet-50 at Class 0, however still there are very much errors in the classes 1 and 2, which needs to be further optimized.

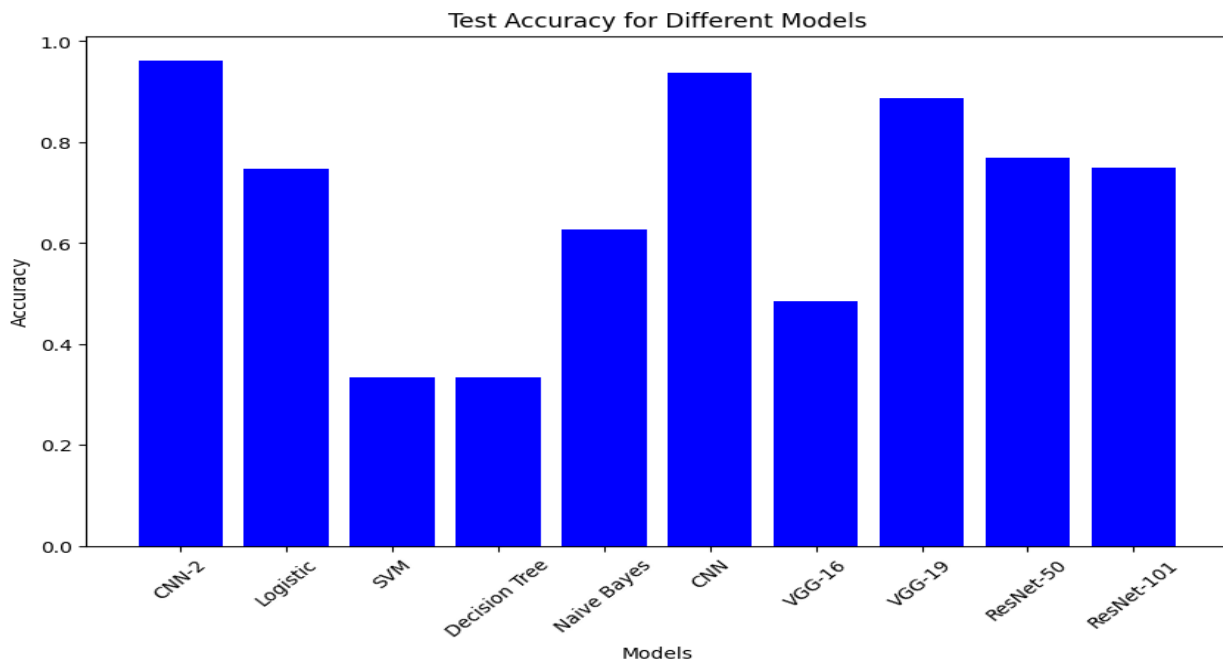


Fig 4.2.21 Bar Graph which shows differences between all models for Lung Cancer

Table 4.2.1: Differences Between All Machine Learning and Deep Learning Models

SNO	Model Name	Accuracy	Loss	Precision	Recall	F1-Score
1	Logistic Regression	74.73%	42.06%	0 – 78% 1 – 88% 2 – 63%	0 – 0.38 1 – 0.99 2 – 0.87	0 – 0.51 1 – 0.93 2 – 0.73
2	SVM	33.33%	66.66%	0 – 20% 1 – 40% 2 – 33%	0 – 0.30 1 – 0.32 2 – 0.87	0 – 0.00 1 – 0.00 2 – 0.50
3	Decision Tree	33.33%	82.12%	0 – 33% 1 – 10% 2 – 0.9%	0 – 1.00 1 – 0.00 2 – 0.00	0 – 0.50 1 – 0.23 2 – 0.61
4	Naïve Bayes	62.69%	42.53%	0 – 47% 1 – 41% 2 – 0.98	0 – 0.90 1 – 0.83 2 – 0.05	0 – 0.64 1 – 0.91 2 – 0.10
5	CNN - 1	93.80%	15.84%	0 – 95% 1 – 91% 2 – 88%	0 – 0.86 1 – 0.98 2 – 0.97	0 – 0.90 1 – 0.99 2 – 0.92
6	VGG-16	57.23%	35.71%	0 – 27% 1 – 46% 2 – 0.96	0 – 0.09 1 – 0.71 2 – 0.73	0 – 0.04 1 – 0.63 2 – 0.83
7	VGG-19	89.30%	14.90%	0 – 88% 1 – 89% 2 – 89%	0 – 0.78 1 – 0.96 2 – 0.92	0 – 0.82 1 – 0.92 2 – 0.91
8	ResNet-50	74.70%	57.90%	0 – 71% 1 – 72% 2 – 78 %	0 – 0.55 1 – 0.92 2 – 0.83	0 – 0.62 1 – 0.86 2 – 0.80
9	ResNet-100	77.32%	55.52%	0 – 65%	0 – 0.67	0 – 0.66

				1 – 78% 2 – 82%	1 – 0.77 2 – 0.82	1 – 0.78 2 – 0.82
10	CNN - 2	96.23%	13.93%	0 – 96% 1 – 99% 2 – 93%	0 – 0.93 1 – 0.97 2 – 0.96	0 – 0.94 1 – 0.95 2 – 0.96

4.3 Covid – 19:

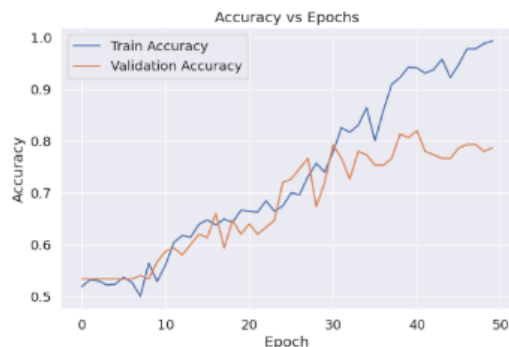


Fig 4.3.1 CNN – 1 Accuracy for COVID – 19.

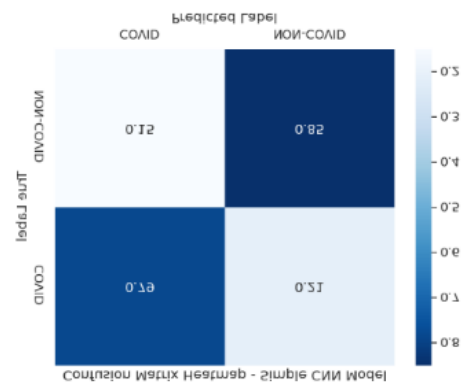


Fig 4.3.2 CNN – 1 Confusion Matrix for COVID – 19.

Fig 4.3.1 depicts the CNN model; the training accuracy grows constantly starting at zero and converging closer to 100% at the 50th epoch, and the validation accuracy moves upward and swings back and forth until finally stabilizing close to 80%, suggesting a good fit on the training data and some margin for smooth generalization. From Fig 4.3.2, the model attains 72% true negative rate and 53% true positive rate, slightly hyper and corresponds to moderate classification performance on classes, and the potential of refinement to reduce overfitting while balancing between class prediction.

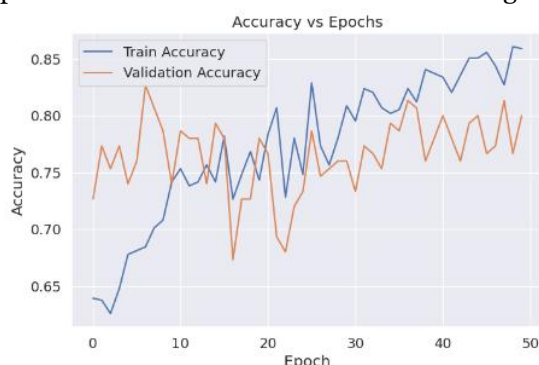


Fig 4.3.3 CNN – 2 Accuracy for COVID – 19.

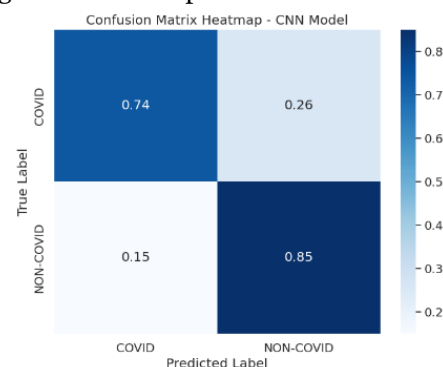


Fig 4.3.4 CNN – 2 Confusion Matrix for COVID – 19.

Fig 4.3.3 shows that after 50 epochs, the optimized CNN model is able to have better division of training and validation accuracy. It asymptotically gets 85%, training accuracy, and the validation accuracy stabilizes, implying that it generalizes better than the initial model. The confusion matrix heatmap, presented in Fig 4.3.4, shows 86% of NON-COVID case classification correct, 74% of COVID case classification correct with false negative and false positive rate of 2:6 and 15:15 respectively. In general, the model works well at differentiating the two classes, with high accuracy.

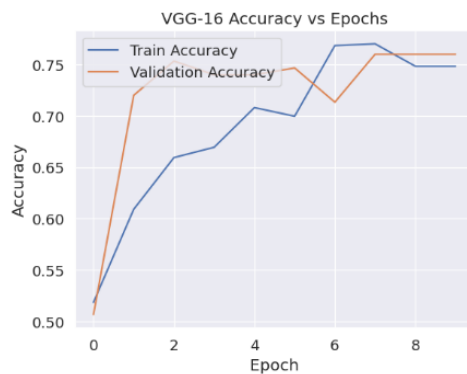


Fig 4.3.5 VGG-16 Accuracy for COVID – 19.

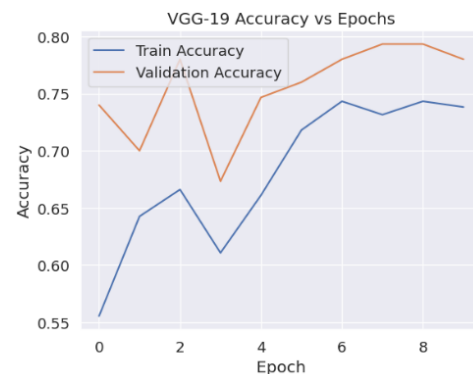


Fig 4.3.6 VGG-19 Accuracy for COVID – 19.

Over time, training accuracy arrives at roughly 75 percent using the VGG 16 model shown in Figure 4.3.5. It was shown that for both tasks, validation accuracy increases rapidly and saturates at roughly the same values as training accuracy, suggesting good model learning with little overfitting. Furthermore in Fig 4.3.6, the validation accuracy of the VGG-19 model also shows gradual growth with regards to the training accuracy, attaining an apex of 75% while it attains around 78%. The validation accuracy is above of the training accuracy and thus does not show any early signal of overfitting, which however is not completely true as there are some fluctuations.

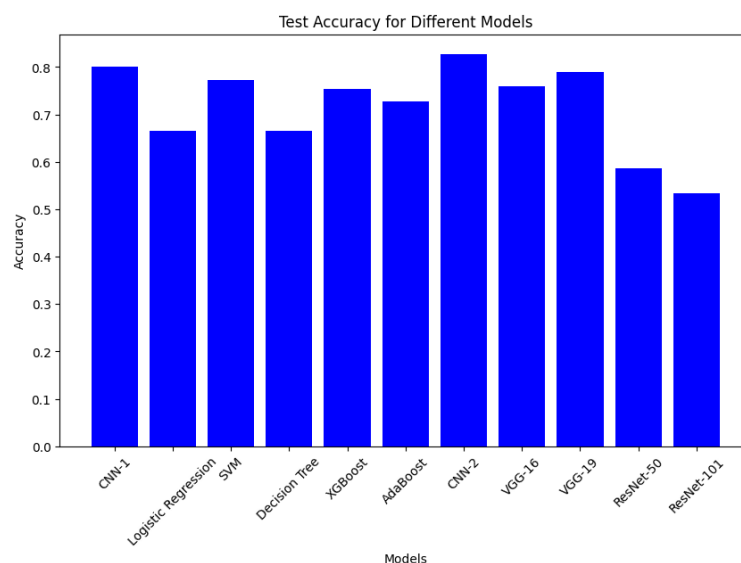


Fig 4.3.7 Bar Graph which shows differences between all models for COVID - 19

Table 4.3.1: Differences Between All Machine Learning and Deep Learning Models

SNO	Model Name	Accuracy	Loss	Precision	Recall	F1-Score
1	Logistic Regression	66.66%	33.33%	0 – 66% 1 – 67%	0 – 0.60 1 – 0.72	0 – 0.63 1 – 0.70
2	SVM	77.33%	22.66%	0 – 75% 1 – 79%	0 – 0.77 1 – 0.78	0 – 0.76 1 – 0.78
3	Decision Tree	66.66%	33.33%	0 – 66% 1 – 67%	0 – 0.66 1 – 0.68	0 – 0.65 1 – 0.58
4	XG - Boost	75.33%	26.39%	0 – 73%	0 – 0.74	0 – 0.74

				1 – 77%	1 – 0.76	1 – 0.77
5	CNN - 1	80.95%	19.70%	0 – 82%	0 – 0.79	0 – 0.80
				1 – 82%	1 – 0.85	1 – 0.83
6	VGG-16	75.99%	25.01%	0 – 81%	0 – 0.63	0 – 0.71
				1 – 73%	1 – 0.88	1 – 0.80
7	VGG-19	77.99%	23.01%	0 – 84%	0 – 0.66	0 – 0.74
				1 – 75%	1 – 0.89	1 – 0.81
8	ResNet-50	58.66%	41.33%	0 – 59%	0 – 0.39	0 – 0.47
				1 – 59%	1 – 0.76	1 – 0.66
9	ResNet-100	53.32%	47.68%	0 – 9%	0 – 0.36	0 – 0.54
				1 – 53%	1 – 0.75	1 – 0.70
10	CNN - 2	83.44%	16.44%	0 – 84%	0 – 0.84	0 – 0.78
				1 – 84%	1 – 0.88	1 – 0.82
11	ADA - Boost	72.66%	27.33%	0 – 72%	0 – 0.67	0 – 0.78
				1 – 73%	1 – 0.78	1 – 0.75

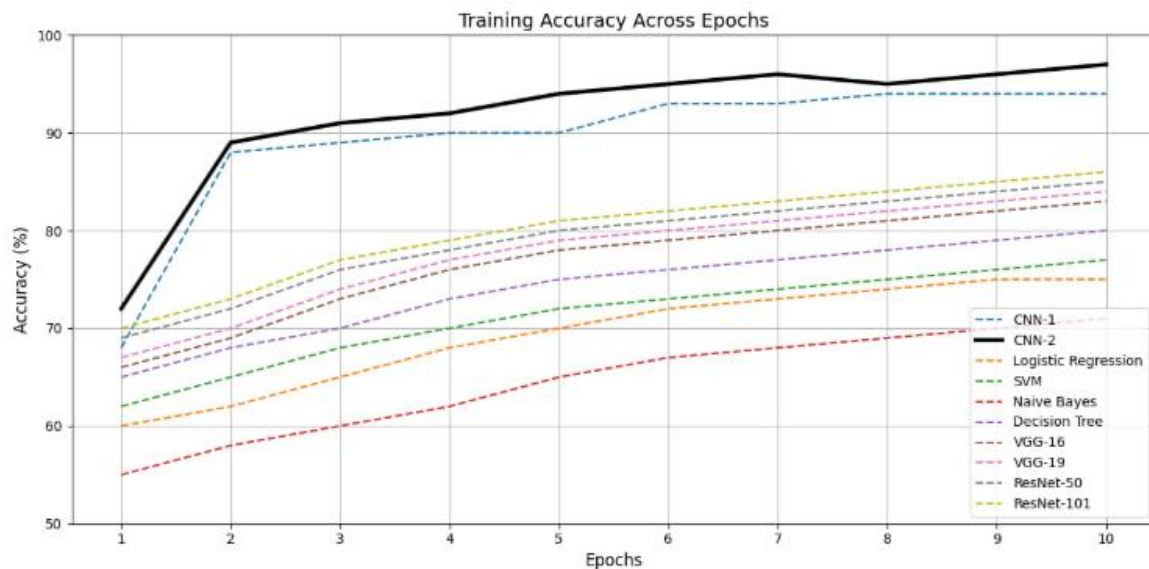


Fig 4.4 All the models training accuracy graph for breast cancer.

This above graph shows training accuracy at various epochs for different machine learning and deep learning models that have been trained on a breast cancer dataset. The inference accuracy increases with the increased number of epochs. From among all the models, the CNN-2 model (thick black line) achieves the highest training accuracy, and comes close to 95%. In addition, CNN-1 also does well with high accuracy above 90%. In the meanwhile, other models such as Logistic Regression, SVM and Naive Bayes have relatively low accuracy improvement and inferior overall performance. An increasing, but stable training accuracy is demonstrated by ResNet-50 and ResNet-101, achieving competitive accuracies against epochs. Decision Tree and Naive Bayes are traditional model, which is quite behind deep learning model.

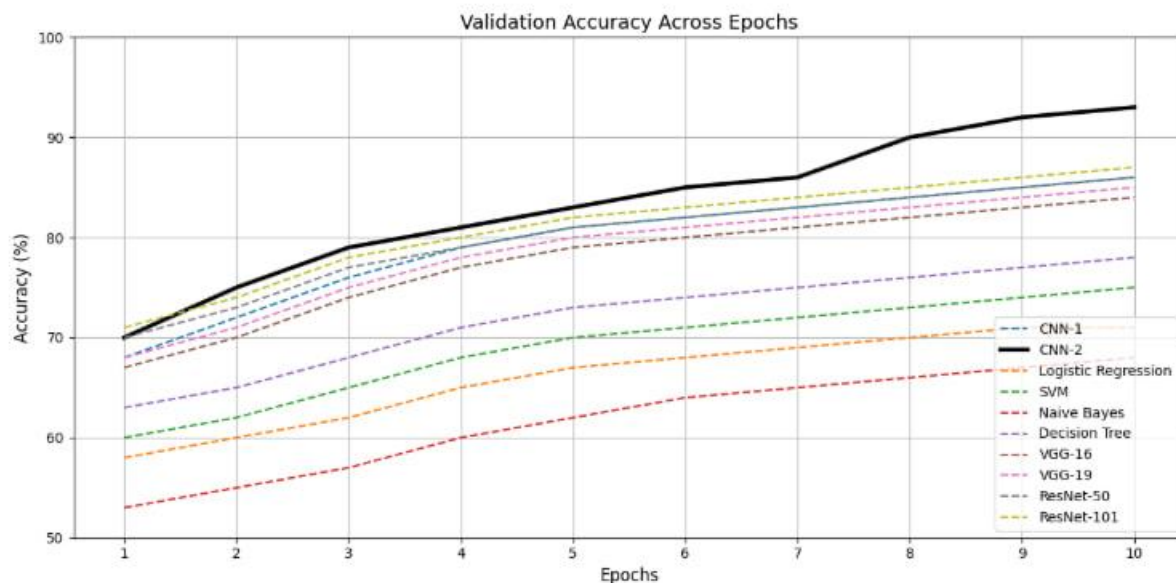


Fig 4.5 All the models validation accuracy graph for breast cancer.

The same set of models were used to generate the above graph, which provides the validation accuracy by epoch. The validation accuracy of CNN-2 and CNN-1 cross 90% after few epochs, although CNN-1 is slightly below CNN-2. ResNet-101 and ResNet-50 show strong results with an even smoothing in results from epoch to epoch. In contrast to that, classical machine learning models such as Logistic Regression, SVM, or Naive Bayes are moderately good but it's even worse as they plateau earlier than deep learning models. Overall validation accuracy for Decision Tree and Naive Bayes remains lower and provides evidence of limited generalization capability.

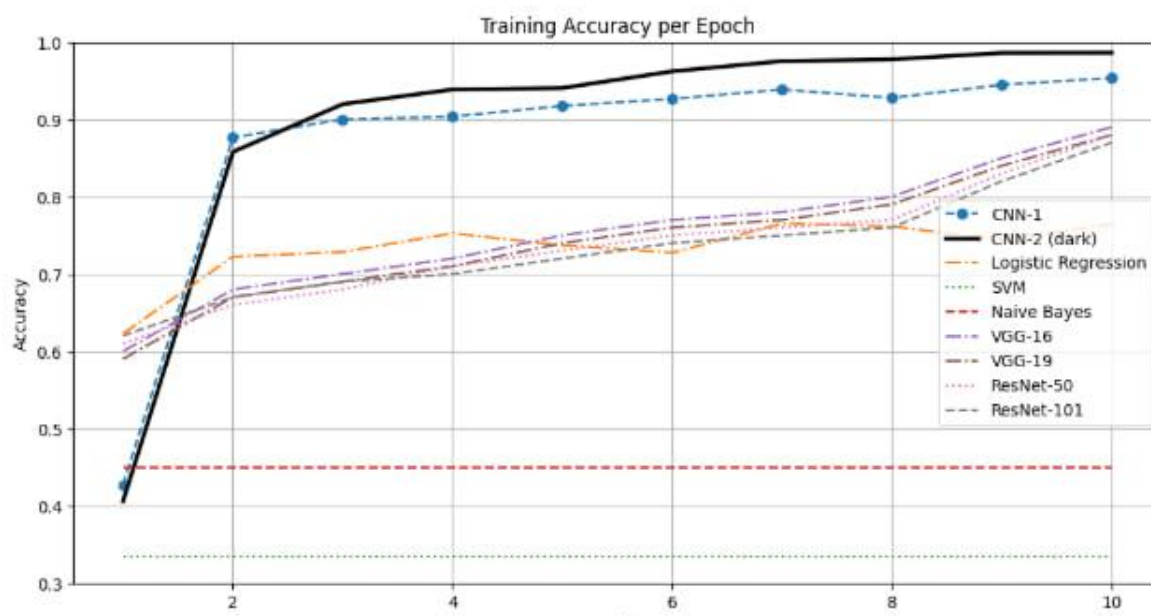


Fig 4.6 All the models training accuracy graph for lung cancer.

Training accuracy at every epoch for several models on a lung cancer dataset is shown by the above graph. CNN-2 gets the highest accuracy with almost 100% after tenth epoch and then CNN-1 with more than 95% accuracy respectively. VGG-16, VGG-19, ResNet-50 & ResNet-101 have steady increasing performance, showing accuracies ranging between 80-90%. On the other hand, Logistic Regression and

SVM will plateau around to 70% – 75%. It's naive Bayes that lags, but the accuracy is barely above 50%. Comparing against traditional methods, this comparison shows that deep learning models perform much better on the task of lung cancer classification.

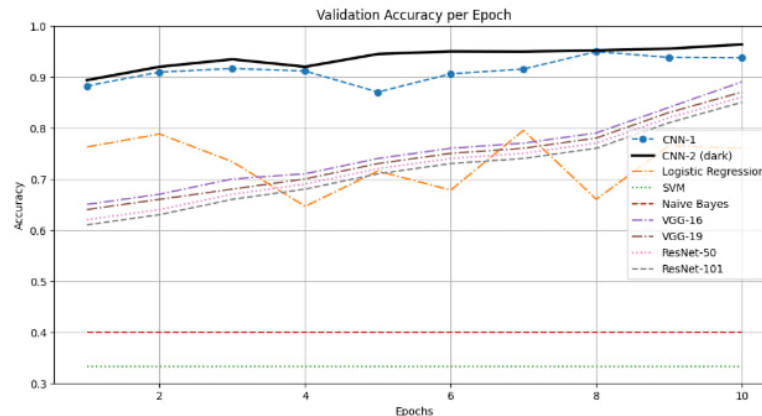


Fig 4.7 All the models validation accuracy graph for lung cancer.

The plot shows the Validation Accuracy per Epoch for these models most probably used for lung cancer detection tasks. Both Convolutional Neural Networks (CNN-1 and CNN-2) are able to achieve high accuracy (>90%-95% respectively in each) with respect to other models, proving their capability to tackle medical imaging data. Validation accuracy is poor below 50%, and Classical models including Logistic Regression, SVM, and Naive Bayes are unable to capture complex patterns. On the other hand, VGG 16, VGG 19, and ResNet 50/101 all show gradual improvement and get up to 85-90 percent accuracy after epoch 10. Among them, ResNet based models slightly outperform VGG model thanks to the deeper layers that help the feature extraction. Overall, CNN based and deep architectures are found to outperform the traditional models for lung cancer detection.

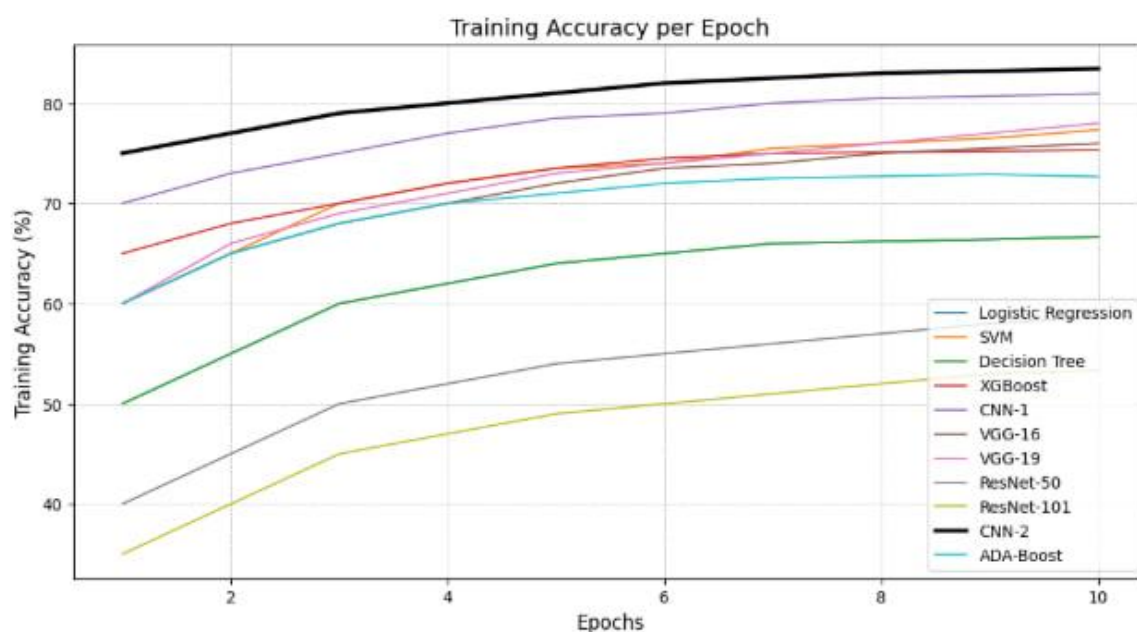


Fig 4.8 All the models training accuracy graph for Covid-19.

The above plot shows Training Accuracy against Epoch for models that may be used for COVID-19 detection. Both CNN-1, CNN-2 and deep learning architectures like ResNet-50, ResNet-101, VGG-16, and VGG-19 achieve the highest training accuracy of 75 to 82 percent through epoch 10, with ResNet-101 and CNN-2 being the best. XGBoost does well, getting around 70% accuracy and since we are working with structured data, it's very efficient. Compared to traditional methods like Logistic Regression, SVM and Decision Tree, they fall short of 60% for complex COVID 19 data. For AdaBoost, we perform the weakest as our performance plateaus at around 50%. I find that deep learning models significantly outperform classical approaches across the board on their ability to deal with high dimensional, complex medical data.

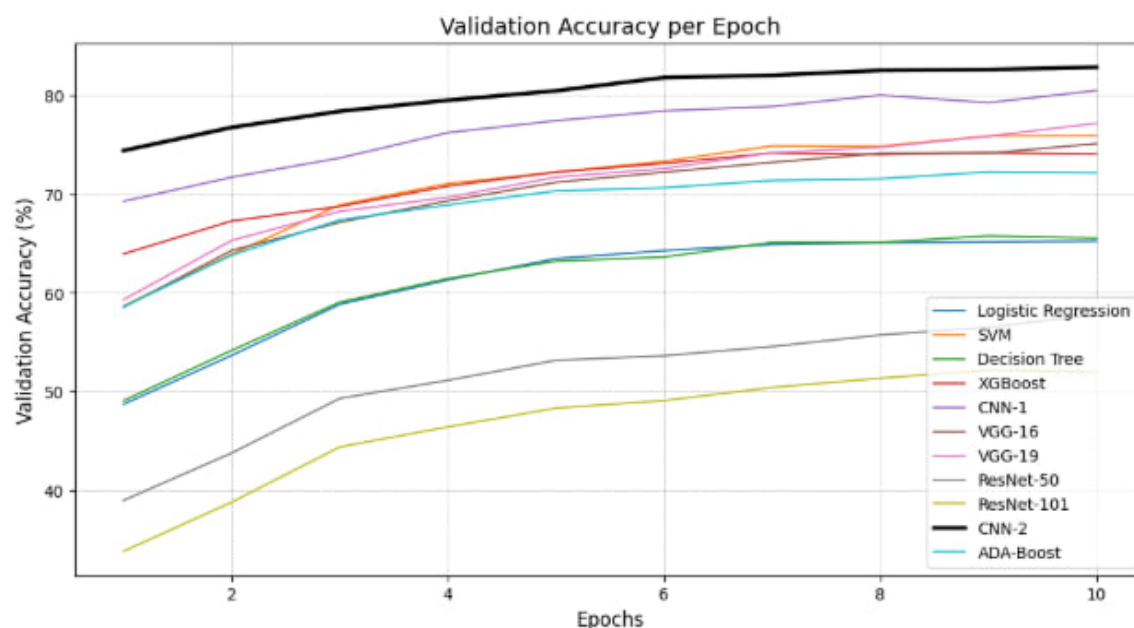


Fig 4.9 All the models validation accuracy graph for covid-19.

The Validation Accuracy per Epoch as the function of applicable models to COVID-19 detection is depicted in the graph. They also found that with epoch 10, CNN-1, CNN-2, ResNet-50, ResNet-101, VGG-16, and VGG-19 give the highest accuracy, which ranged from 75% to 80%. CNN-2, with 80% accuracy, and ResNet-101, with 78% accuracy, are second and first, respectively. Its strength in handling complex data is shown when XGBoost finds good around 70--75% accuracy. However, when compared to traditional methods like Logistic Regression, SVM or Decision Tree, moderate performance of around 60% – 65% is retained. It can be seen that for ADA-Boost, performance plummets below 50% whereby it shows its limits. In general, deep learning methods outperform the traditional approaches and demonstrate their capability of performing the COVID-19 detection tasks.

5. CONCLUSION:

Different machine learning to classify breast cancer, lung cancer and COVID-19 images with their distinguishing features. While Logistic Regression, SVM and Decision Tree were able to handle smaller dataset of cancer such as breast cancer in a satisfactory manner, advanced methods such as XG Boost and Ada Boost over showed better modeling for imbalanced data. By virtue of their capability of capturing complex patterns within CT and mammography images, deep learning architectures such as CNN, VGG-16, VGG-19, ResNet-50 and ResNet-101, were of greater utility for lung cancer and COVID prediction. All these models were deployed for the image rich datasets, and CNN and some of its more complex variants (CNN-2, VGG, and ResNet) improved accuracy significantly over traditional models. Interestingly, the deep learning methods – CNN-2 and VGG-19 – tend to have high classification accuracy in lung cancer and COVID-19 datasets. Model performance is compared to offer the advantage

of feature extraction and data augmentation combined with deep learning in classification accuracy. Nevertheless, in real world applications, the trade off with model complexity, computational cost and performance is crucial.

6. FUTURE WORK:

Further development and improvement is possible in several areas, including the look ahead. With respect to diagnoses such as breast cancer, lung cancer and COVID 19, there may be potential to improve model accuracy by further adding data, such as data from MRI scans and clinical data, that could be combined with image based diagnostic. Furthermore, further work could study additional advanced architectures, including transformers, and hybrid models that can achieve more efficient feature extraction and classification. Moreover, transfer learning and few shot learning could be applied to decrease training time as well as enhance model's generalization, even when the dataset is small or large. Further, the adoption of XAI solutions to develop explainable AI (XAI) solutions may be necessary to achieve interpretability of model decisions necessary for subsequent clinical adoption. Finally, we would integrate the real time prediction models into clinical workflows; we would develop strong frameworks for cross validation (CV) between multiple datasets and institutions to assess: 1) generalization performance in the ability of the models to generalize across independent datasets or institutions for cancer detection and COVID detection.

REFERENCES:

- [1] Sun YS, Zhao Z, Yang ZN, Xu F, Lu HJ, Zhu ZY, Shi W, Jiang J, Yao PP, Zhu HP. Risk Factors and Preventions of Breast Cancer. *Int J Biol Sci.* 2017 Nov 1;13(11):1387-1397. doi: 10.7150/ijbs.21635. PMID: 29209143; PMCID: PMC5715522.
- [2] Pamela Cowin, Tracey M Rowlands, Sarah J Hatsell, Cadherins and catenins in breast cancer, *Current Opinion in Cell Biology*, Volume 17, Issue 5, 2005, Pages 499-508, ISSN 0955-0674, <https://doi.org/10.1016/j.ceb.2005.08.014>.
- [3] M. Veta, J. P. W. Pluim, P. J. van Diest and M. A. Viergever, "Breast Cancer Histopathology Image Analysis: A Review," in *IEEE Transactions on Biomedical Engineering*, vol. 61, no. 5, pp. 1400-1411, May 2014, doi: <https://doi.org/10.1109/TBME.2014.2303852>.
- [4] A. M. Hassan and M. El-Shenawee, "Review of Electromagnetic Techniques for Breast Cancer Detection," in *IEEE Reviews in Biomedical Engineering*, vol. 4, pp. 103-118, 2011, doi: <https://doi.org/10.1109/RBME.2011.2169780>.
- [5] E. C. Fear, P. M. Meaney and M. A. Stuchly, "Microwaves for breast cancer detection?," in *IEEE Potentials*, vol. 22, no. 1, pp. 12-18, Feb.-March 2003, doi: <https://doi.org/10.1109/MP.2003.1180933>.
- [6] Z. Wang *et al.*, "Breast Cancer Detection Using Extreme Learning Machine Based on Feature Fusion With CNN Deep Features," in *IEEE Access*, vol. 7, pp. 105146-105158, 2019, doi: <https://doi.org/10.1109/ACCESS.2019.2892795>.
- [7] R. Roslidar *et al.*, "A Review on Recent Progress in Thermal Imaging and Deep Learning Approaches for Breast Cancer Detection," in *IEEE Access*, vol. 8, pp. 116176-116194, 2020, doi: <https://doi.org/10.1109/ACCESS.2020.3004056>.
- [8] S. B. Sakri, N. B. Abdul Rashid and Z. Muhammad Zain, "Particle Swarm Optimization Feature Selection for Breast Cancer Recurrence Prediction," in *IEEE Access*, vol. 6, pp. 29637-29647, 2018, doi: <https://doi.org/10.1109/ACCESS.2018.2843443>.
- [9] Y. Yari, T. V. Nguyen and H. T. Nguyen, "Deep Learning Applied for Histological Diagnosis of Breast Cancer," in *IEEE Access*, vol. 8, pp. 162432-162448, 2020, doi: <https://doi.org/10.1109/ACCESS.2020.3021557>.

- [10] M. Liu *et al.*, "A Deep Learning Method for Breast Cancer Classification in the Pathology Images," in *IEEE Journal of Biomedical and Health Informatics*, vol. 26, no. 10, pp. 5025-5032, Oct. 2022, doi: <https://10.1109/JBHI.2022.3187765>.
- [11] S. S. Raoof, M. A. Jabbar and S. A. Fathima, "Lung Cancer Prediction using Machine Learning: A Comprehensive Approach," *2020 2nd International Conference on Innovative Mechanisms for Industry Applications (ICIMIA)*, Bangalore, India, 2020, pp. 108-115, doi: <https://10.1109/ICIMIA48430.2020.9074947>.
- [12] A. Mohammadi *et al.*, "Lung Cancer Radiomics: Highlights from the IEEE Video and Image Processing Cup 2018 Student Competition [SP Competitions]," in *IEEE Signal Processing Magazine*, vol. 36, no. 1, pp. 164-173, Jan. 2019, doi: <https://10.1109/MSP.2018.2877123>.
- [13] R. P.R., R. A. S. Nair and V. G., "A Comparative Study of Lung Cancer Detection using Machine Learning Algorithms," *2019 IEEE International Conference on Electrical, Computer and Communication Technologies (ICECCT)*, Coimbatore, India, 2019, pp. 1-4, doi: 10.1109/ICECCT.2019.8869001.
- [14] Z. Li *et al.*, "Deep Learning Methods for Lung Cancer Segmentation in Whole-Slide Histopathology Images—The ACDC@LungHP Challenge 2019," in *IEEE Journal of Biomedical and Health Informatics*, vol. 25, no. 2, pp. 429-440, Feb. 2021, doi: <https://10.1109/JBHI.2020.3039741>.
- [15] S. H. Hawkins *et al.*, "Predicting Outcomes of Non-small Cell Lung Cancer Using CT Image Features," in *IEEE Access*, vol. 2, pp. 1418-1426, 2014, doi: <https://10.1109/ACCESS.2014.2373335>.
- [16] N. S. Nadkarni and S. Borkar, "Detection of Lung Cancer in CT Images using Image Processing," *2019 3rd International Conference on Trends in Electronics and Informatics (ICOEI)*, Tirunelveli, India, 2019, pp. 863-866, doi: <https://10.1109/ICOEI.2019.8862577>.
- [17] F. Taher and R. Sammouda, "Lung cancer detection by using artificial neural network and fuzzy clustering methods," *2011 IEEE GCC Conference and Exhibition (GCC)*, Dubai, United Arab Emirates, 2011, pp. 295-298, doi: <https://10.1109/IEEEGCC.2011.5752535>.
- [18] D. P. Kaucha, P. W. C. Prasad, A. Alsadoon, A. Elchouemi and S. Sreedharan, "Early detection of lung cancer using SVM classifier in biomedical image processing," *2017 IEEE International Conference on Power, Control, Signals and Instrumentation Engineering (ICPCSI)*, Chennai, India, 2017, pp. 3143-3148, doi: <https://10.1109/ICPCSI.2017.8392305>.
- [19] X. Wang *et al.*, "Weakly Supervised Deep Learning for Whole Slide Lung Cancer Image Analysis," in *IEEE Transactions on Cybernetics*, vol. 50, no. 9, pp. 3950-3962, Sept. 2020, doi: <https://10.1109/TCYB.2019.2935141>.
- [20] J. Alam, S. Alam and A. Hossan, "Multi-Stage Lung Cancer Detection and Prediction Using Multi-class SVM Classifier," *2018 International Conference on Computer, Communication, Chemical, Material and Electronic Engineering (IC4ME2)*, Rajshahi, Bangladesh, 2018, pp. 1-4, doi: <https://10.1109/IC4ME2.2018.8465593>.
- [21] M. Jamshidi *et al.*, "Artificial Intelligence and COVID-19: Deep Learning Approaches for Diagnosis and Treatment," in *IEEE Access*, vol. 8, pp. 109581-109595, 2020, doi: <https://10.1109/ACCESS.2020.3001973>.
- [22] X. Wang *et al.*, "A Weakly-Supervised Framework for COVID-19 Classification and Lesion Localization From Chest CT," in *IEEE Transactions on Medical Imaging*, vol. 39, no. 8, pp. 2615-2625, Aug. 2020, doi: <https://10.1109/TMI.2020.2995965>.

[23] Y. Pathak, P. K. Shukla and K. V. Arya, "Deep Bidirectional Classification Model for COVID-19 Disease Infected Patients," in *IEEE/ACM Transactions on Computational Biology and Bioinformatics*, vol. 18, no. 4,

[24] S. A. -F. Sayed, A. M. Elkorany and S. Sayed Mohammad, "Applying Different Machine Learning Techniques for Prediction of COVID-19 Severity," in *IEEE Access*, vol. 9, pp. 135697-135707, 2021, doi: <https://10.1109/ACCESS.2021.3116067>.

[25] M. J. Horry *et al.*, "COVID-19 Detection Through Transfer Learning Using Multimodal Imaging Data," in *IEEE Access*, vol. 8, pp. 149808-149824, 2020, doi: <https://10.1109/ACCESS.2020.3016780>.